Quaternary Science Reviews 211 (2019) 59–72

Contents lists available at ScienceDirect

Quaternary Science Reviews

journal homepage: www.elsevier.com/locate/quascirev

Forest and lake dynamics in response to temperature, North American monsoon and ENSO variability during the Holocene in Colorado (USA)

Gonzalo Jiménez-Moreno [a, *], R. Scott Anderson [b], Bryan N. Shuman [c], Ethan Yackulic [b]

[a] Departamento de Estratigrafía y Paleontología, Universidad de Granada, Fuente Nueva s/n, 18002, Granada, Spain
[b] School of Earth & Sustainability, Northern Arizona University, Flagstaff, AZ, 86011, USA
[c] Department of Geology and Geophysics, University of Wyoming, Laramie, WY, 82071, USA

ARTICLE INFO

Article history:
Received 14 December 2018
Received in revised form
4 March 2019
Accepted 9 March 2019
Available online 21 March 2019

ABSTRACT

Learning how terrestrial environments responded to past temperature and precipitation variations can help anticipate how these environments will respond to natural climate variability upon which human induced climate change is superimposed. Here we present a detailed multi-proxy analysis of a sediment core from Emerald Lake, located at the montane-subalpine forest transition in west-central Colorado. The record tracks changes in the lake environment, vegetation and fire activity mostly related to climate change for the latest Pleistocene and Holocene, and complements the previously published lake-level reconstruction from the same site. Vegetation and lake level show similar patterns with insolation changes and other regional paleoclimate records for temperature, with coldest conditions during the Younger Dryas (YD), warming in the early Holocene - thermal maximum reached around 6800 cal yr BP – and cooling in the middle and late Holocene. This record also shows how subalpine environments reacted to Holocene moisture dynamics for both summer, related to the North American Monsoon (NAM), and winter precipitation that could be associated with El Niño Southern Oscillation (ENSO), indicating that Emerald Lake was sensitive to long-term and millennial-scale regional and global climate changes. Climatic perturbations, generally cold and/or arid events and low lake levels at ca. 8200, 4200, 1200-1000 cal yr BP influenced the vegetation around Emerald Lake in association with well-known worldwide climatic events.

1. Introduction

High-elevation montane and subalpine forests dominated by *Pinus contorta* (lodgepole pine), *Picea engelmannii* (Engelmann spruce) and *Abies lasiocarpa* (subalpine fir) represent one of the dominant forest types in western North America, covering ~2.9 million ha (http://csfs.colostate.edu/colorado-forests/forest-types/; Lotan and Critchfield, 1990) in Colorado's Rocky Mountains alone. These forests are highly valued natural resources, for they are critical in trapping and slowly releasing snow-water for drinking supplies, represent an important source of wood products, contain critical habitat for threatened species and are important in recreational activities (Leatherman, 2008). During past millennia, a primary influence on long-term vegetation changes in Rocky Mountain forests has been changing climate (Fall 1997; Cairns and Malanson, 1998), but changes in fire regime have also been important, with fire event frequency strongly linked to climate variability (Power et al., 2008; Carter et al., 2017). In the last few decades, these relationships have become intensified, as these forests have been dramatically impacted by ecosystem disturbances (Romme et al., 2006), including drought (Cook et al., 2015; McDowell and Allen, 2015; Williams et al., 2015), widespread severe fires (Moritz et al., 2012; Dennison et al., 2014; Jolly et al., 2015) and insect infestation (Sturrock et al., 2011), perhaps driven in part by anthropogenic climate change (Mathys et al., 2017). Investigating the forest and lake responses to past climatic events can help in anticipating how these environments will respond to natural climate variability upon which human induced climate change is superimposed.

This study was undertaken to further investigate changes in subalpine and montane forests during the Holocene within the core of Colorado's high mountainous region. Initially, climatic changes were inferred from lake-level fluctuations indicated by the sedimentary record at our site, Emerald Lake, a small lake in west-

* Corresponding author.
E-mail address: gonzaloj@ugr.es (G. Jiménez-Moreno).

https://doi.org/10.1016/j.quascirev.2019.03.013

central Colorado, which was previously analyzed by Shuman et al. (2014). Their climatic reconstruction documented relatively low lake levels for most of the early and middle Holocene, with a substantial rise after ~5700 cal yr BP. Using this climatic record as our starting point, we ask a research question related to these climatic changes: How have climate changes, such as those documented by the lake-level record and by other regional evidence of temperature and precipitation changes, impacted forest composition and disturbances, such as fire?

To this end, we compared a detailed fossil pollen record from Emerald Lake with a multi-proxy record of the local climate and disturbance changes (magnetic susceptibility, hyperspectral sediment analysis, the previously published lake-level data, and charcoal analysis). The lake-level history provides a record of effective precipitation based on direct sedimentary evidence of past shoreline positions based on multiple sediment cores and ground penetrating radar (GPR) data from Emerald Lake (Shuman et al., 2014). This comparison permits us to determine how sedimentation, vegetation and lake hydrology responded to the same environmental forcings, mostly climate, in the region. Possible climatic controls on the water availability in the study area during the Holocene are: (1) orbital-scale driven changes in insolation controlling temperature and evapotranspiration (Shuman, 2012); (2) multi-century shifts in the position of Pacific storm tracks, which likely changed with influences such as ENSO (Donders et al., 2008; Barron and Anderson, 2011; Anderson, 2012); and (3) changes in summer precipitation associated with centennial-and millennial-scale oscillations in North American Monsoon (NAM) regimes related with latitudinal movements of the Intertropical Convergence Zone (ITCZ) (Haug et al., 2001; Poore et al., 2005). However, some studies have noted that summer precipitation is not effective, for it evaporates during the hot summer months, being mostly consumed by vegetation and unable to do the groundwater recharge necessary to allow lakes to expand (Antinao and McDonald, 2013; Menking et al., 2018). These previous studies call for greater winter moisture in order to raise lake levels. It may be possible to reveal the relative importance of different seasonal moisture regimes on environmental change over time by coupling a paleovegetation record to an independently determined lake level history (based on shorelines) in an area that is influenced by all the above mentioned controls on the water availability.

In the study area today, upper and lower treeline boundaries, with tundra-like vegetation above and steppe below, occur between around 3600 and 2800 m in elevation, respectively. Therefore, the pollen stratigraphy from Emerald Lake at 3050 m elevation should be sensitive to changes in the composition of subalpine and montane communities and the elevation of upper and lower treeline, which are primarily dependent on the length and relative warmth of the growing season (upper treeline) and the strength of summer monsoon and the more effective winter precipitation (lower treeline) (Fall 1997). Alternatively, changes in seasonal temperatures may also be important in long-term vegetation change, due to cold air drainage in mountain valleys (Coop and Givnish, 2008), such as HalfMoon Valley where Emerald Lake is found. The comparison of these multiproxy data with other paleoclimate records helps to disentangle the effects of temperature and precipitation dynamics (North American Monsoon (NAM) vs. winter precipitation including ENSO) in the high-elevation environments from the southern Rockies throughout the Holocene.

2. Study site

Emerald Lake (39°09′06″ N, 106°24′22″ W; 3051 m asl) is a small (~1.26 ha; 4.5 m maximum depth) kettle lake located ~19 km southwest of Leadville, Lake County, Colorado (Shuman et al., 2014, Fig. 1). The lake fills a depression in a valley bottom along Halfmoon Creek, situated between Mt. Massive to the north and Mt. Elbert to the south. Emerald Lake sits in hummocky outwash between two Pinedale-age (last glacial period) lateral moraines, which originated from an outlet glacier in the Sawatch Range (Nelson and Shroba, 1998). Pinedale deposits are underlain by older glacial deposits (Nelson and Shroba, 1998; Shuman et al., 2014) with bedrock consisting of Precambrian biotite gneisses, migmatites and granites of the Elbert and Massive massifs (Tweto et al., 1978). Previous study by Shuman et al. (2014) has documented that the lake level has fluctuated through time, but when visited in July of 2007, the maximum depth of the lake was ~4.2 m.

Central Colorado is influenced both by winter storms originating from the Pacific and thus influenced by factors such as ENSO, and summer convective storms influenced by subtropical air masses, the NAM (Wise, 2012). Shuman et al. (2014) documented the importance of sites such as Emerald Lake, which presently sit in a transition zone between the region of positive October–April correlations of Southern Oscillation Index to the north, and of negative correlations to the south. The two closest climate stations to Emerald Lake are Leadville (3252 m; 15.1 km NE) and Twin Lakes (2752 m; 10.5 km SE) (WRCC website, accessed 11 September 2018). Average annual high and low temperatures for both of these sites are similar (9.2 vs 10.7° C, and −5.8 vs. −5.4° C, respectively). But average precipitation and snowfall differ markedly (39.5 vs. 24.4 cm, and 269.9 vs. 114.3 cm, respectively), demonstrating the importance of local effects, particularly altitude, on precipitation.

Modern vegetation in the southern Rocky Mountains of central Colorado is characterized by alpine and upland herb communities above ~3500 m, high-elevation subalpine and montane conifer forest with *Populus tremuloides* (quaking aspen) above ~2900-2800 m, and *Artemisia* (sagebrush) steppe below this (Lagenheim, 1962). The subalpine *Picea engelmannii* (Engelmann spruce) − *Abies lasiocarpa* (subalpine fir) community is best developed locally between 3200 and 3500 m but can occur as low as ~2590 m and as high as ~3800 m as patches of krummholz (Lagenheim, 1962; personal observations). Dominant trees are *Picea engelmannii* and *Abies lasiocarpa*, but *Populus tremuloides* and *Pinus contorta* var. *latifolia* (lodgepole pine) can be locally common. A montane forest mostly made up of *Pinus contorta* but also *Picea pungens* (Colorado blue spruce), *Pseudotsuga menziesii* (Douglas fir), *Pinus ponderosa* (ponderosa pine), *Quercus gambellii* (gamble oak) and *Populus tremuloides* (quaking aspen) occurs below the subalpine forest. *Pinus edulis* (Colorado piñon)—*Juniperus monosperma* (oneseed juniper) woodlands occur on the lower slopes of the range from ~2400 to 1800 m. Isolated stands of *P. edulis* occur within 50 km southeast and northwest of Emerald Lake (Charles Truettner, personal communication, 2012; http://swbiodiversity.org/seinet/taxa). *Artemisia* (sagebrush) steppe occurs below this. The sagebrush steppe community, which occurs primarily along the Arkansas River valley and south-facing lower mountain slopes, is dominated by *Artemisia tridentata* (big sagebrush) and *Chrysothamnus* spp. (rabbitbrush) at an elevation of 2800 m.

Emerald Lake itself is located within the montane forest vegetation belt, which is dominated locally around the lake by dense stands of *P. contorta*. *Picea engelmannii* and *Abies* sp., as well as *Populus tremuloides* rarely occur. Though the sandy soils of the understory are generally sparse, shrubs include *Shepherdia canadensis* (buffalo-berry), *Juniperus communis* (common juniper), *Vaccinium myrtillis* (myrtle blueberry), *Pentaphylloides floribunda* (shrubby cinquefoil), *Arctostaphylos uva-ursi* (kinnikinnik), *Rosa woodsii* (rose), *Linnaea borealis* (twinberry), *Ribes parviflora* (thimbleberry), and *Mahonia repens* (Oregon-grape). Herbs include

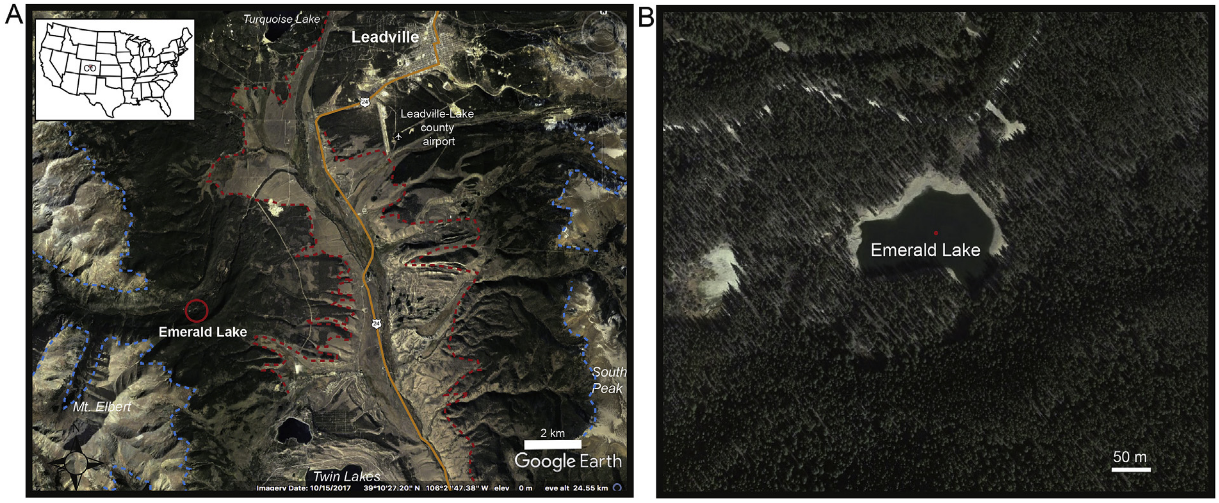

Fig. 1. Location of Emerald Lake, Colorado (A) and coring location (B). Dashed blue and red lines show upper and lower treeline, respectively. Aerial photos taken from Google Earth (http://www.earth.google.com).

Thalictrum sp. (meadow-rue), *Solidago* sp. (goldenrod), *Pyrola minor* (lesser wintergreen), *Antennaria parvifolia* (pussytoes), *Epilobium angustifolium* (fireweed), *Achillea lanulosa* (yarrow) and *Trifolium* sp. (clover). Shrubs around the lake are dominated by *Salix* sp. (Terminology from Weber, 1976).

3. Materials and methods

Two sediment cores were collected in July 2007, including a 299 cm-long core, from 15 to 314 cm depth (EL 07-02) using a Livingstone square-rod piston corer, and a short core (EL 07-01), using a plexiglass tube, which included the unconsolidated upper 22.5 cm of sediments. They were retrieved within a meter of each other in the deepest part of Emerald Lake. The two cores overlap and were correlated visually using slight sediment color changes. The Livingstone core was split into halves, photographed, described, and scanned for magnetic susceptibility and hyperspectral image analysis. The short core was sectioned into whirlpak bags. Both cores were sampled for pollen and radiometric dating at the Laboratory of Paleoecology (LOP), Northern Arizona University.

The Emerald Lake core chronology was developed using a combination of ^{210}Pb and ^{137}Cs activity profile of the upper sediments of core 07-01 [by Doug Hammond (USC)], and nine calibrated AMS radiocarbon dates from core 07-02 (UCIAMS and Direct-AMS; Table 1; Fig. 2). Sediments for ^{210}Pb activity profile were ground and subsequently were placed in plastic tubes for gamma counting, using a well-type intrinsic Ge detector. ^{210}Pb was determined from its 46 keV peak, ^{226}Ra by a weighted average of its daughter peaks (^{214}Pb at 295 and 352 keV, ^{214}Bi at 609 keV), and ^{137}Cs from its 662 keV peak. ^{226}Ra results were corrected for radon loss, determined to be 7% of the total, based on measurement of radon released from similar samples and from the standard. Standardization was based on reference materials supplied by the EPA. Excess ^{210}Pb was calculated by subtracting ^{226}Ra activity from total ^{210}Pb. The excess ^{210}Pb in the upper portion of the EL 07-01 (0–8 cm) could be adequately fit with an exponential function, which was done with the program Kaleidagraph. The depth attenuation coefficient (b) for the profile was used to estimate a linear accumulation rate s:

$$s = \lambda/b$$

where $\lambda = {}^{210}$Pb day constant (1/y) and b = depth attenuation coefficient (1/cm).

Organic material for AMS dates consisted of leaf fragment, seed and wood-charcoal samples (Table 1). Samples for AMS dating were

Table 1
Age data for the studied sedimentary record from Emerald Lake, Colorado.

Laboratory number[a]	Real Depth (cm)	Material dated	Dating method	Age (14C cal yr BP ± 1σ)	Calibrated age (cal yr BP) 2σ range	Median age (cal yr BP)
	0		Present	AD2007	−57	−57
D. Hammond	5	Bulk sediment	210 Pb	AD1963	−13	−13
UCIAMS-62792	30.6	Leaf fragments	^{14}C	390 + 25	326–508	470
D-AMS 028,240	57.2	Leaf fragments	^{14}C	1823 + 44	1624–1868	1760
UCIAMS-62793	81.7	Leaf fragments	^{14}C	2760 + 20	2786–2921	2850
D-AMS 028,241	113.5	Needle and leaf fragments	^{14}C	3049 + 52	3079–3376	3254
UCIAMS-62794	144.2	Leaf fragments	^{14}C	4650 + 25	5313–5464	5408
UCIAMS-62795	185.8	Leaf fragments	^{14}C	5985 + 25	6748–6888	6824
D-AMS 028,242	213.5	Leaf fragments & mixed seeds	^{14}C	6448 + 78	7179–7507	7363
D-AMS 028,243	246.1	Seeds, needle and wood fragments	^{14}C	7322 + 64	8005–8311	8124
UCIAMS-62796	276.8	Wood, charcoal	^{14}C	9770 + 30	11,175–11238	11,208

Note: All ages were calibrated using CALIB 7.10 (Stuiver and Reimer, 1993).
[a] Sample number assigned at radiocarbon laboratory; UCIAMS = University of California at Irvine W.M. Keck Carbon Cycle Accelerator Mass Spectrometry Laboratory; D-AMS = Direct Accelerator Mass Spectrometry radiocarbon dating service, Bothell, Washington.

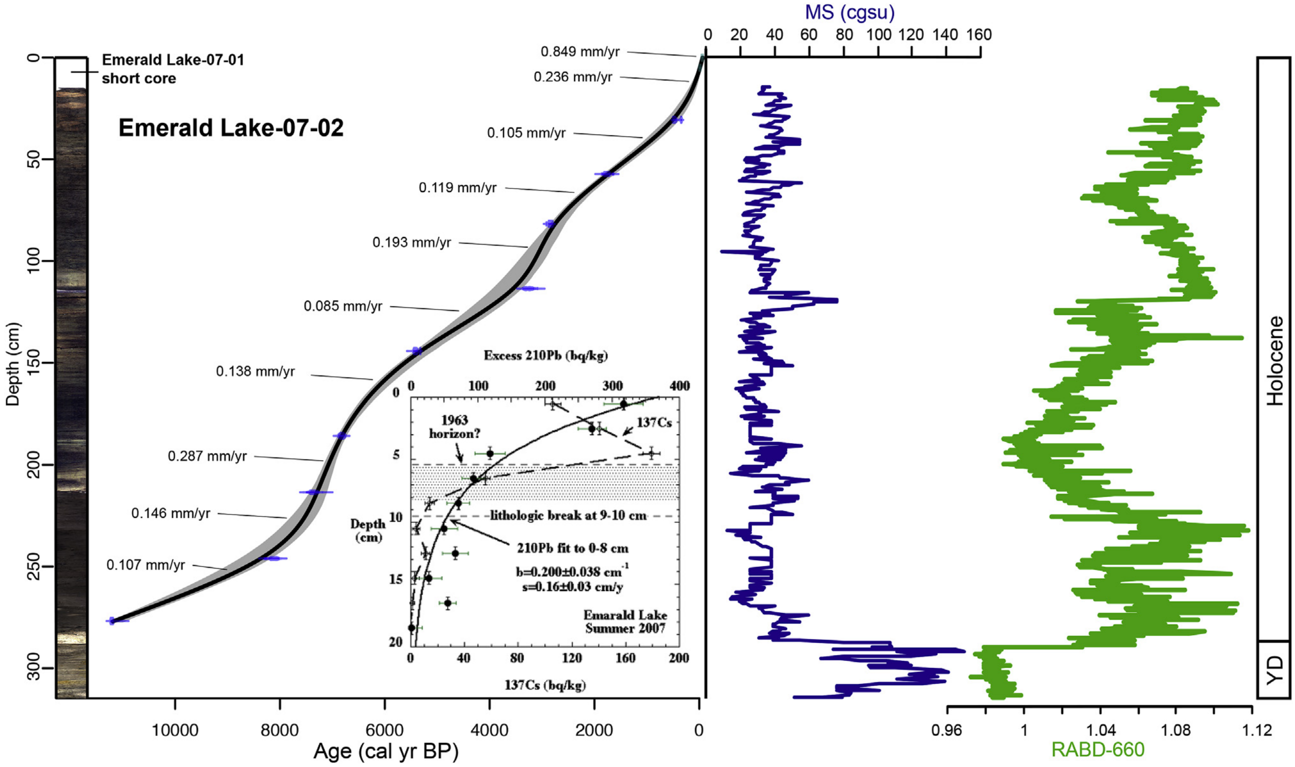

Fig. 2. Sedimentary record, age-depth diagram obtained by Clam software (Blaauw, 2010) including the ^{210}Pb and ^{137}Cs (bq/kg) profiles, magnetic susceptibility (MS) and RABD$_{660}$ data for the Emerald Lake record. Sediment accumulation rates (SAR) between radiocarbon dates are shown. Note that the topmost part of the sedimentary record (short core 07-01) is not shown due to the impossibility of splitting the unconsolidated sediments into halves, precluding it to be photographed.

initially dried and weighed before submission. Radiocarbon dates were converted to calendar year before present (cal yr BP) using the IntCal13 curve (Reimer et al., 2013) with Calib 7.10 (http://calib.qub.ac.uk/calib/) (Table 1). The age model for the Emerald Lake record (Fig. 2) was built with Clam 2.2 (Blaauw, 2010) using smooth spline (type = 4) with spar = 0.3 (smooth). Sediment accumulation rates (SARs) were calculated between the radiocarbon and ^{210}Pb-^{137}Cs dates using the age model provided by Clam 2.2.

Lithology (Fig. 2) and wet Munsell color were described from split core segments in the laboratory. Magnetic susceptibility (MS), a measure of the tendency of sediment to carry a magnetic charge (Snowball and Sandgren, 2001), was measured with a Bartington MS2E meter in dimensionless cgs units (cgsu; Fig. 2). Measurements were taken directly from the core surface every 0.5 cm for the entire length of EL 07-02 core.

Hyperspectral analyses were used to determine potential changes in lake paleoproductivity through time. These analyses were performed for the Livingstone core using a Specim SISU single core scanner with a sCMOS-50-V10E spectral camera, following the methodology outlined by Yackulic (2017). These analyses are possible because substances interact differently with different wavelengths of radiation, absorbing (reflecting) more energy in certain narrow regions of the spectrum known as absorption (reflectance) bands (Yackulic, 2017). Absorption bands may therefore be diagnostic of specific materials (Butz et al., 2015). Diagnostic absorption bands in the visible to near infrared (VNIR) range are generally limited to photopigments such as chlorophylls and carotenoids that have distinct reflectance minima in the blue to near infrared range (Scheer, 2006). Absorption band measurements can also be calibrated to quantify the relative amount of a substance (Butz et al., 2015). Relative absorption band depth (RABD) calculations have been widely used for quantitative pigment estimations, most notably in measurements of the reflectance trough related to chlorophyll *a* and its diagenetic products at 660–670 nm (e.g., Rein and Sirocko, 2002; Trachsel et al., 2010; Butz et al., 2015). Therefore, RABD$_{660}$ is a strong indicator of lacustrine primary production and plant organic matter. This analysis has advantages with respect to other proxies for organic matter (e.g., LOI) because it indicates a specific type of organic matter such as chlorophyll and because it is higher resolution with far less necessary labor. Image preprocessing and normalization followed the routine developed by Butz et al. (2015). Spectral data were binned to a 1 mm resolution (depth) for comparison with other proxies. Spectral indices were calculated in R version 3.4.3.

Fifty-four samples (1 cm^3) were analyzed for pollen analysis at a resolution of about 4–6 cm (ca. 200-yrs) between samples (Fig. 3). Pollen extraction methods followed a modified Faegri and Iversen (1989) methodology. Counting was performed at 400× magnification to a minimum pollen sum of 300 terrestrial pollen grains. Fossil pollen grains were compared with their present-day relatives using published keys and the modern pollen reference collection at Northern Arizona University. *Pinus* pollen was divided into four categories: diploxylon (locally, *P. contorta* or *P. ponderosa*), haploxylon (bristlecone, *P. aristata*; limber, *P. flexilis*), *P. edulis* (piñon) and indeterminate (Jacobs, 1985). *Pinus* pollen grains were classified as haploxylon if verrucae were present on the leptoma and as diploxylon if verrucae were not present. Haploxylon grains with a grain length of less than 65 µm were considered *P. edulis*, while those greater than 65 µm were simply considered 'haploxylon'. The pollen results were plotted in a detailed diagram (Fig. 3). Relative percentages of terrestrial pollen taxa were calculated not including aquatic taxa such as Cyperaceae, *Typha*, *Potamogeton*, *Nuphar* or

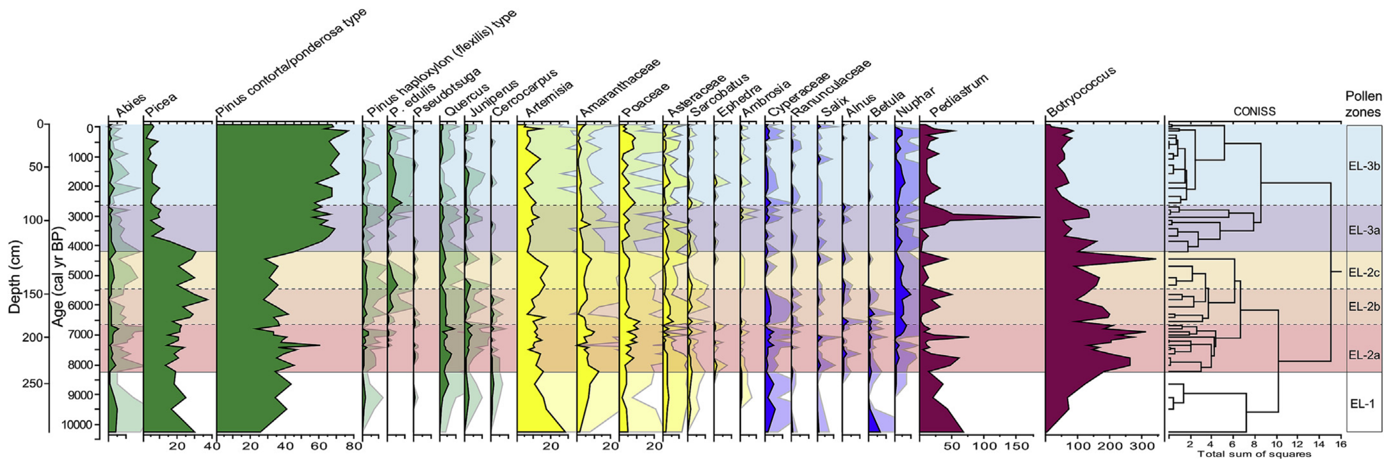

Fig. 3. Pollen diagram of the Emerald Lake record showing percentages of selected taxa (higher than 1%). Trees and shrubs are represented in green, herbs in yellow. The aquatics, in blue (including *Alnus*, *Betula*, *Salix*, Cyperaceae, Liliaceae, Ranunculaceae and *Thalictrum*) were excluded from the total pollen sum. Percentages of algae (*Pediastrum* and *Botryococcus*), in purple, were calculated with respect to the terrestrial pollen sum. The zonation was made using cluster analysis provided by CONISS (Grimm, 1987). Lighter shading shows x5 exaggeration of the plots.

Myriophyllum. Percentages of the aquatic algae *Botryococcus* and *Pediastrum* were calculated with respect to the total terrestrial pollen. The pollen zonation was done by cluster analysis of the pollen percentages using CONISS (Grimm, 1987) and visual inspection. A group with the sum of the relative percentages of montane thermophilous species such as *Quercus*, *Juniperus* and *Cercocarpus* was made. Percentages of Arboreal Pollen (AP) and Non-Arboreal Pollen (NAP) and the AP/NAP ratios were also calculated. These are useful indicators of forest density (Faegri and Iversen, 1989). Several other pollen ratios were calculated to determine changes in the vegetation related with climate. The ratio of *Picea* to *Pinus* (S/P ratio) mostly points to treeline elevation change in the area and the *Artemisia* to *Picea* (A/P) or *Picea* to *Artemisia* (P/A) ratio to relative shifts between the subalpine and the lower altitudinal steppe vegetation belts, respectively. These ratios have been used in previous studies (e.g., Maher, 1963; Toney and Anderson, 2006; Jiménez-Moreno et al., 2011; Johnson et al., 2013) to infer paleoenvironmental change and estimate past climate conditions by calculating relative abundances of significant climate-sensitive pollen types.

Charcoal analysis (unpublished) was carried out in a previously retrieved parallel sedimentary core, Emerald Lake core H also taken from the deepest part of the basin in 2005 (Shuman et al., 2014). The Emerald Lake-07–02 and H cores can be correlated using their independent MS and absolute age information (Fig. 4) and charcoal data can be used to infer past fire activity in the Emerald Lake area. Samples for charcoal analysis were taken every 1 cm down the length of core H. The 1 cm^3 sub-samples were soaked in 6% hydrogen peroxide for 24 h and wet sieved using a 125 μm screen. All charcoal pieces larger than 125 μm were then counted using a stereomicroscope at 10–40× magnification. Charcoal counts for each sample were converted to charcoal influx (CHAR; number of charcoal particles per cm^2 per year; Fig. 4). Magnetic susceptibility, loss-on-ignition, and sand content were also measured in core H to aid correlation among cores; the sand content was determined as the percent of the dry sediment mass composed of mineral grains >63 μm, based on wet sieving and subsequent LOI of the coarse fraction. As described previously by Shuman et al. (2014), Emerald Lake core H was dated using 11 AMS ^{14}C ages. To provide a chronology for the sedimentary charcoal record, samples ages were estimated using Bchron (Parnell et al., 2008; Shuman et al., 2014).

4. Results

4.1. Chronology and sedimentary rates (SAR)

The age-depth model for the 314 cm of this new Emerald Lake record was built using 10 absolute dates (both ^{14}C and ^{210}Pb) and suggests that this record continuously covers at least the last ca. 11,200 cal yr BP (Table 1; Fig. 2). The uppermost part of the Emerald record (EL 07-01) was dated using maximum ^{210}Pb and ^{137}Cs activity, signaling an age of AD 1963 at ~5 cm depth (D. Hammond, pers. comm.; Fig. 2). The ^{210}Pb data from 0 to 8 cm was used to calculate accumulation rate. The fit to the ^{210}Pb profile in the upper 8 cm indicates a depth attenuation coefficient of 0.200 ± 0.038 per cm, yielding an accumulation rate of 0.16 ± 0.03 cm/yr. The predicted depth of the maximum in ^{137}Cs is at 7 cm, slightly deeper than the best estimate based on the ^{137}Cs profile. The sample from 5 to 6 cm was not counted, and its analysis might define the position of the maximum more precisely. The depth of the 1963 horizon predicted from excess ^{210}Pb at 5 cm is indicated by the stippled zone in Fig. 2, and is reasonably concordant with the horizon chosen from the ^{137}Cs profile.

Nine radiometric dates with median ages from 470 to 11,208 cal yr BP provide age information for the rest of the Holocene record (Table 1; Fig. 2). The SAR is fairly constant, with average values between 0.1 and 0.3 mm/yr throughout the record (Fig. 2). Changes in SAR coincide with lithological changes, increasing with detrital content (MS). SAR increased in the uppermost part of the record with values around 0.849 mm/yr at the top. This increase in SAR is consistent with the flocculent, non-compacted nature of sediments at the top of lake sediment cores. The changes in SAR are broadly consistent with the patterns observed for core H (Shuman et al., 2014).

4.2. Lithology and magnetic susceptibility (MS)

Sediments from Emerald Lake are primarily inorganic in the lowermost portion of the core, becoming more organic towards the top (Fig. 2). The EL-07-02 core bottoms at 314 cm with banded light and dark sands up to 290 cm. These sediments are overlain by transitional facies towards more organic content, with sandy clays and sandy gyttja between 290 and 263.5 cm. Very organic dark brown gyttja, peaty in places, characterize the rest of the sequence

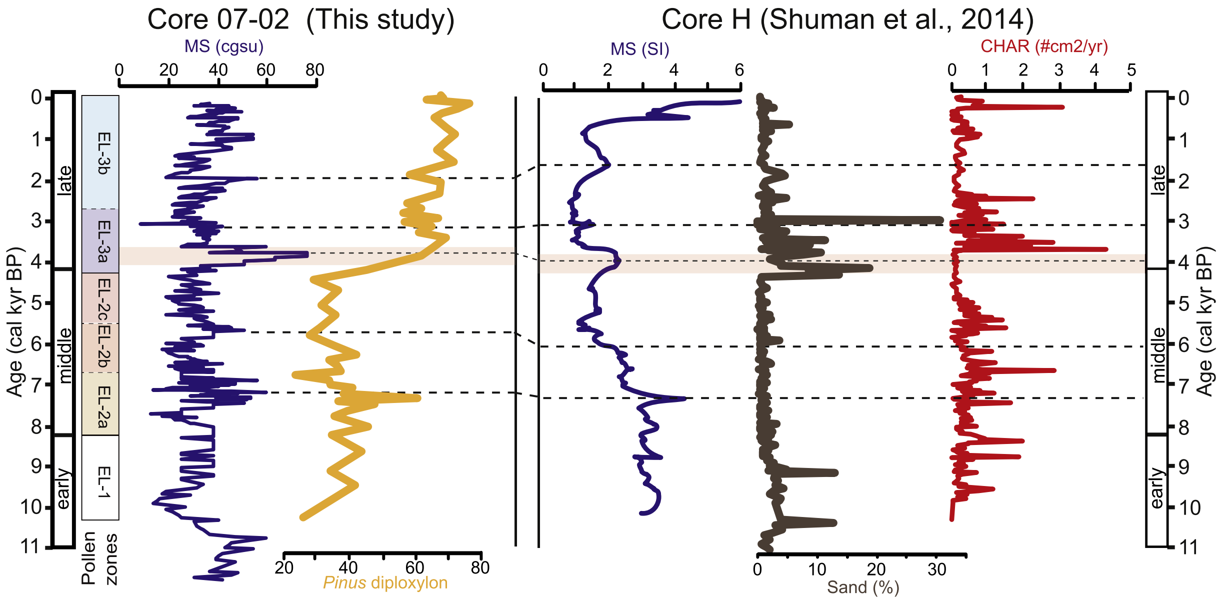

Fig. 4. Comparison and correlation between Emerald Lake cores 07–02 and H (Shuman et al., 2014). MS was used for correlations (dashed lines). A significant event of change in the vegetation and the lake environment is marked by a pink shading around 4000 cal yr, when a significant drop in the lake level, deduced by peaks in MS and sand in the sediment cores, occurred during a time when *Pinus* diploxylon (*P. contorta*) boosted and completely occupied the area. Associated with the increase in *P. contorta* in the area is an increase in fire activity, pointing to *P. contorta* tree-fire association. This event could be related with the well-known 4.2 ka climatic event.

up to 9 cm. Lighter-color and slightly more inorganic sediments occur between 215 and 185 cm and between 150 and 110 cm. Another change in color occurs in the uppermost 50 cm of the record, with a change towards gray silty gyttja in the topmost 9 cm of core EL-07-02 between total depths below the sediment-water interface of 24–15 cm. The topmost 15 cm of the record, recovered in core 07-01 are characterized by dark brown gyttja.

MS data vary between 150 (290 cm; 12,300 cal yr BP extrapolated) and 10 cgsu (96 cm; 3060 cal yr BP) (Fig. 2). Highest MS values characterize the bottom and mostly inorganic part of the record between 314 and 284 cm (latest Pleistocene, most likely YD until ca. 11,800 cal yr BP). Holocene MS values oscillate between 60 and 20 cgsu with a mean value of 34 cgsu and dark organic sediments corresponding with relatively low MS and lighter and more inorganic sediments to relatively high MS. Peaks in MS above the mean occur between 9000 and 8000, 7500–6600, 5500, 4200–3500, 2500–2000, 1200–900 and 500-200 cal yr BP. Differences exist in the MS of core 07-02 and core H, but both show prominent maxima at ca. 7300 and 4200-3500 cal yr BP. The latter coincides with a peak in the sand content of core H, which is associated with a period of low water levels (Shuman et al., 2014).

4.3. Hyperspectral analysis $RABD_{660}$ data

Several studies have previously confirmed that $RABD_{660}$ is a reasonable estimate of variability in chlorophyll(chl) *a* abundance, and therefore, an indicator of total productivity (Das et al., 2005; Wolfe et al., 2006; Michelutti and Smol, 2016). Considerable variability exists in $RABD_{660}$ values over the entire record (Fig. 2). During the YD, $RABD_{660}$ values are less than 1, suggesting a complete absence of chlorophyll in the sediment. In general, $RABD_{660}$ values are consistently higher prior to ca. 7800 cal yr BP, lowest but increasing during most of the middle Holocene to ca. 3700 cal yr BP, with consistently highest values during the late Holocene. Low $RABD_{660}$ values occur during maxima in MS. This negative relationship can be clearly seen in the YD part of the record but also in the $RABD_{660}$ minima, for example at around 7000, 4000 and 2100 cal yr BP.

4.4. Pollen analysis

The bottom inorganic part of the Emerald Lake record reported here is barren of pollen and the first analyzed pollen sample comes from 268 cm depth (10,250 cal yr BP). Decreasing but high relative NAP values around 30% characterize the early and middle Holocene (low AP/NAP ratios; Fig. 5). The AP during this period is mostly depicted by *Picea* and *P. contorta-ponderosa*. A substantial increase in AP, and thus in AP/NAP ratios, occurs in the late Holocene mostly due to the expansion in *P. contorta*. Objective zonation of the pollen data by CONISS cluster analysis and visual examination suggests three pollen zones with subdivisions (EL-1 to EL-3; Fig. 3). The major clusters identified by CONISS (represented by the split between zones EL-2 and EL-3 at 4200 cal yr BP) capture this sharp contrast in older pollen assemblages represented by >20% *Picea* pollen, <50% *Pinus* pollen, and >10% *Artemisia* and younger assemblages dominated by *Pinus* pollen (>65%) with low amounts of *Picea* and non-arboreal taxa. Additional changes in the relative abundances of the taxa form the basis for further differentiating the Holocene pollen zones.

Zone EL-1 [~10,250 to ~8200 cal yr BP (268-244 cm depth)]. EL-1 encompasses the early Holocene and is dominated by pollen of *Artemisia*, *Picea* and *Pinus* diploxylon type, most likely *P. contorta* (lodgepole pine), the dominant type of pine in the area today. Since *P. contorta* and *P. ponderosa* (ponderosa pine) pollen are indistinguishable, *P. ponderosa* is also possible. This zone is characterized by the highest percentage of *Artemisia* (around 30%) and *Abies* (~5%) in the entire record, a peak in *Picea* (around 30%) and an increase in *P. contorta* type from a minimum of ~25%–40%. Amaranthaceae pollen percentages show an increasing trend in this zone from about 1.5 to 10%. Maximum values in Cyperaceae, around 5%, are reached in this zone. The aquatic algae *Pediastrum* and *Botryococcus* are both present in this zone, showing opposite trends in their occurrences, decreasing and increasing, respectively.

Zone EL-2 [~8200 to ~4200 cal yr BP (244-120 cm depth)]. Zone EL-2, with three subzones, features the highest percentages of *Picea*, *Abies*, *Quercus*, *Juniperus*, *Cercocarpus*, Amaranthaceae and *Sarcobatus* as well as the highest occurrence of aquatics, such as

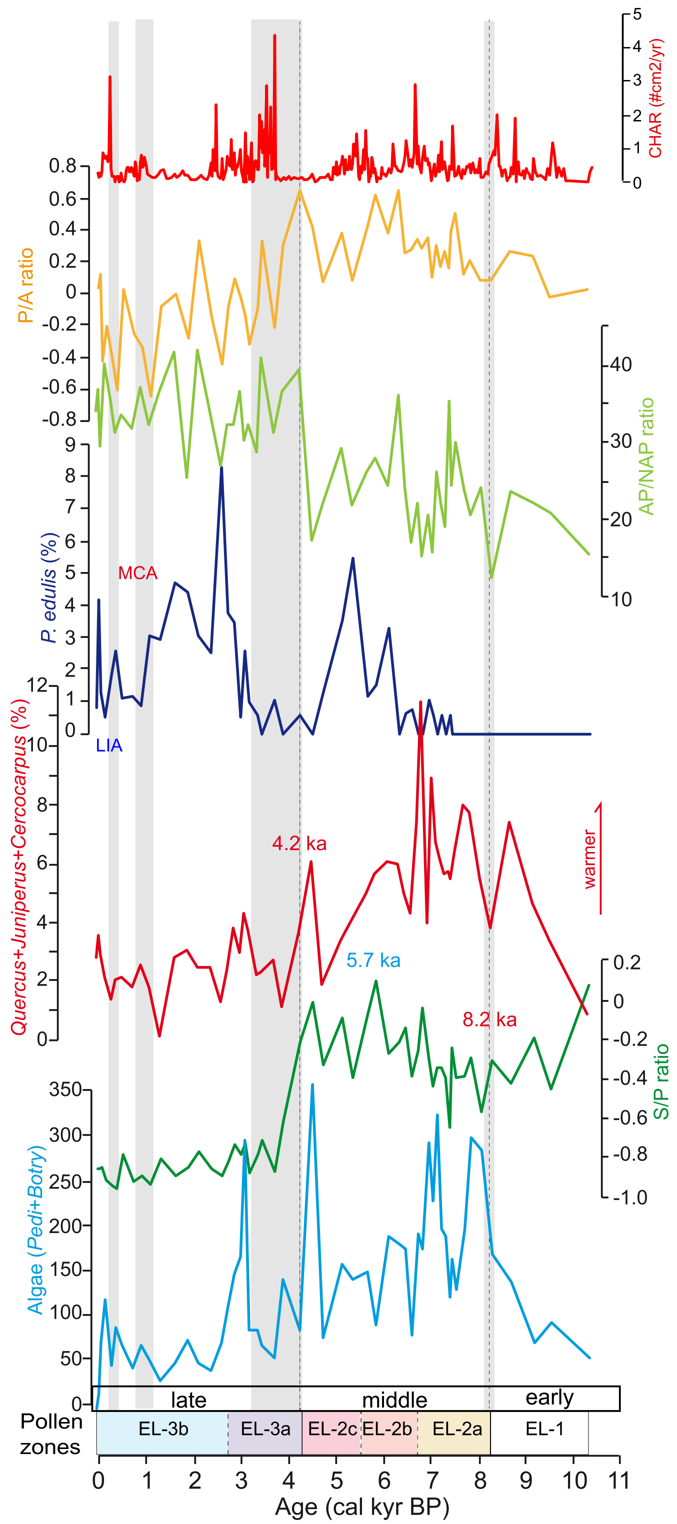

Fig. 5. Emerald Lake pollen ratios and taxa used as paleoclimate proxies in this study (see text for explanation). P/A, S/P and AP/NAP stand for *Picea* to *Artemisia*, *Picea* (spruce) to *Pinus* and arboreal pollen to non-arboreal pollen ratios, respectively. Pollen zones are shown at the bottom. Dashed lines mark the boundaries between early, middle and late Holocene stages following Walker et al. (2012). Gray shadings highlight millennial-scale changes in the vegetation and lake environment due to climatic changes discussed in the text and following figures. MCA and LIA stand for Medieval Climate Anomaly and Little Ice Age, respectively. Red and blue color for 8.2, 5.7, 4.2 MCA and LIA means arid or humid periods, respectively.

Nuphar and *Botryococcus*. EL-2a [~8200 to 6700 cal yr BP (244-180 cm depth)] is characterized by an increasing trend in *P. contorta* (and/or *P. ponderosa*) and a zonal maximum of ~60% reached at ~7300 cal yr BP. *Picea* is also abundant, showing slight variations in its occurrences in the zone around 20%. The subzone is also characterized by the highest occurrences of *Quercus*, *Juniperus*, *Cercocarpus*, *P.* haploxylon (*P. flexilis*) type and Poaceae and the lowest occurrences in *P. contorta* type. Two peaks in *Botryococcus* and *Pediastrum* algae are recorded at around 7800 and 7000 cal yr BP.

The highest occurrences of *Picea* in the entire record (38%) at 5800 cal yr BP and relatively low abundances of *P. contorta* characterize EL-2b [~6700 to 5500 cal yr BP (206-145 cm depth)]. The subzone also contains the highest occurrence of *Nuphar*. Subzone EL-2c [~5500 to 4200 cal yr BP (145-120 cm depth)] contains a peak in *P. edulis* pollen percentages (~5300 cal yr BP). *Artemisia* increases and then decreases at the end of this subzone. This subzone depicts the last peak in algae (mostly *Botryococcus*) at ~4450 cal yr BP.

Zone EL-3 [~4200 cal yr BP to Present (120-0 cm depth)]. The most significant change observed in the Holocene record is the dramatic increase in *P. contorta* type at the base of zone EL-3, with high abundances of this pollen type (averaging ~65%) defining the zone. *Picea* suffered a sharp decrease at the base of the zone as did aquatic (Cyperaceae, *Nuphar* and *Botryococcus*), *Quercus*, *Artemisia*, and Amaranthaceae pollen percentages. Zone EL-3 is subdivided into two subzones. EL-3a [~4200 to 2600 cal yr BP (120-76 cm depth)] depicts comparatively low occurrence of *P. contorta* type, but higher *Picea* and *Botryococcus* and *Pediastrum* algae compared to subzone EL-3b [~2600 cal yr BP to Present (76–0 cm depth)]. *P. edulis* shows the highest occurrence at the beginning of the EL-3b subzone (~2550 cal yr BP) and a decreasing trend with some variations until Present. *P. contorta* exhibits a slight increasing trend in this subzone, contrary to *Picea*, which shows the opposite.

4.5. Charcoal analysis

CHAR varies between 0 and 4.3 particles cm^{-2} yr^{-1} (Fig. 4). Little CHAR is recorded during the early Holocene (pollen zone EL-1) and shows a slight increasing trend towards the end of this period with peaks at ~8800 and 8400 cal yr BP. The middle Holocene (pollen zone EL-2) is characterized by multiple CHAR oscillations with peaks at ~7500, 6700 and between 5600 and 5400 cal yr BP, and very low CHAR in the middle-late Holocene transition between 4900 and 3700 cal yr BP. The rest of the late Holocene (pollen zone EL-3) is characterized by a CHAR maximum reached at 3770 cal yr BP and relatively high values with a decreasing trend between 3770 and 2600 cal yr BP, and another peak that occurred at ~2470 cal yr BP. Low values are recorded between 2300 and 1100 cal yr BP and two oscillations are observed in the last millennium with maxima reached at ~1000–900 and 200-80 cal yr BP, and minima at ~500-300 and the last ~80 cal yr BP.

5. Discussion

Pollen records from high-elevation alpine lakes and bogs from the Rocky Mountains have proven to be sensitive to climate changes during the late glacial and early Holocene (Carrara et al., 1984; Reasoner and Jodry, 2000; Toney and Anderson, 2006; Anderson et al., 2008a, b; Shuman et al., 2009; Jiménez-Moreno et al., 2008, 2011; Briles et al., 2012; Jiménez-Moreno and Anderson, 2012a; Higuera et al., 2014). Treeline boundaries respond to changes in both temperature and precipitation (Fall 1997; Cairns and Malanson, 1998) and vegetation belt movements during the Holocene have been recognized palynologically from changing pollen percentages and pollen ratios. In these studies, upper and lower treeline oscillations most-likely point to long-

term and millennial-scale climatic variations. Here we used the *Picea/Artemisia* ratios (P/A ratios) and the *Picea*/total *Pinus* ratio (spruce/pine, or S/P ratio; Fig. 5) as proxies for the elevation of treeline and the density of *Picea* subalpine forest (sensu Carrara et al., 1984; Toney and Anderson, 2006; Jiménez-Moreno et al., 2011). Thermophilous montane taxa such as *Quercus*, *Juniperus* and *Cercocarpus* indicate elevational shifts of the lower forest-steppe ecotone through time mostly controlled by climate, especially temperature (Neilson and Wullstein, 1983; Fall 1997). Increases in *Artemisia*, mostly occurring today below lower treeline, can be explained as a warming- and drying-induced upslope elevational displacement of the steppe (Jiménez-Moreno et al., 2011; Jiménez-Moreno and Anderson, 2012a). $RABD_{660}$ hyperspectral data have been shown to be a good estimate of chl *a* and chlorin concentration and thus a proxy for algal productivity and plant organic matter in lake sediments (Grosjean et al., 2014). It is likely that most of the $RABD_{660}$ signal has an aquatic source, for terrestrial material would have to be deposited almost immediately after the death of the source plant due to rapid chlorophyll degradation (von Gunten et al., 2009). Here we compare the Emerald Lake multi-proxy record to other paleoclimate records from the area and globally to obtain information about possible triggers for environmental changes.

5.1. Late glacial environments

The Emerald Lake basin is situated between two Pinedale-age moraines in HalfMoon Valley (Nelson and Shroba, 1998). Although these moraines are currently undated, recent cosmogenic ^{10}Be exposure ages of moraine boulders from the Pinedale glaciation in the upper Arkansas River valley at Twin Lakes, just 11 km southeast of Emerald Lake (see Fig. 1), show average ages of 21.8 ± 0.7 ka for the last glacial maximum (Schweinsberg et al., 2016). The exact timing of local late-glacial glacier recession is unknown, and age estimates for deglaciation in the southern Rockies range from ~19,400 (the end of the Last Glacial Maximum) to 11,500 cal yr BP (the end of the Younger Dryas), probably depending on an individual site's elevation and orientation (Andrews et al., 1975; Benson et al., 2005; Toney and Anderson, 2006; Guido et al., 2007; Briles et al., 2012; Jiménez-Moreno and Anderson, 2012a; Johnson et al., 2013). Shuman et al. (2014) showed that the glacial kettle basin that contains Emerald Lake was completely deglaciated and that the lake had begun to form sometime before ~15,900-15225 cal yr BP. However, this lower part of their record is associated with low net sediment accumulation rates (<4 cm/ka) before ~11,000 cal yr BP and may indicate only intermittent or seasonal standing water in the basin before the beginning of the Holocene (Shuman et al., 2014). Very inorganic light-color sandy and clayey facies with highest MS and lowest $RABD_{660}$ values pointing to minimal productivity recorded in our EL 07-02 core may be consistent with this interpretation. Unfortunately, pollen data are not available from these sediments, perhaps due to poor preservation, but its absence is consistent with our interpretation of an intermittently dry basin.

The evidence of a shallow or intermittently dry Emerald Lake basin during the late Pleistocene is also consistent with evidence of widespread low lake levels at other sites across the Rockies from 15,000 to 11000 cal yr BP (Shuman and Serravezza, 2017) and may represent the Terminal Pleistocene Drought recorded by speleothems (e.g., Polyak et al., 2012). Likewise, the high abundance of non-arboreal taxa, such as *Artemisia*, in the lowest pollen samples in zone EL-1 indicates an open, semi-arid landscape during the earliest Holocene, which may have persisted since the late Pleistocene (Figs. 2–3).

Previous pollen studies in the area show that vegetation during the late glacial was characterized by low percentages of arboreal pollen and high *Artemisia* steppe, herbs and grasses implying that tundra and *Picea* parkland occurred in the area and that average temperatures were significantly colder than later on during the Holocene (Legg and Baker, 1980; Jiménez-Moreno et al., 2011; Briles et al., 2012; Jiménez-Moreno and Anderson, 2012a; Johnson et al., 2013). Climatic oscillations during the Bølling-Allerød interstadial and Younger Dryas (YD) stadial are recorded in the pollen record from Tiago Lake (Jiménez-Moreno et al., 2011; ~200 km to the north) and Cumbres Bog (Johnson et al., 2013; ~300 km to the south) through increases and decreases in the arboreal content indicating warming and cooling, respectively. High-elevation studies from the southern Rockies show a downslope displacement of the subalpine vegetation of several hundred meters during the YD (Markgraf and Scott, 1981; Fall 1997; Reasoner and Jodry, 2000; Toney and Anderson, 2006; Jiménez-Moreno et al., 2008, 2011). The Emerald Lake record appears to capture an increase in forest cover after the YD related to warming (see below).

5.2. Early Holocene

The early Holocene is characterized in the Emerald Lake pollen record by a rapid climate warming. The area near the lake was dominated by *Picea* and *Abies* parkland with *Artemisia* between ~10,500 and 8200 cal yr BP (zone EL-1; Fig. 3). The occurrence of *Artemisia* steppe elements in the vegetation indicates that continued relatively cold and arid conditions prevailed. Similar vegetation has been interpreted from other high elevation pollen records from central Colorado (Tiago Lake – Jiménez-Moreno et al., 2011; Kite Lake – Jiménez-Moreno and Anderson, 2012a), southward to the San Juan and Sangre de Cristo mountains (Little Molas Lake – Toney and Anderson, 2006; Hunters Lake – Anderson et al., 2008a; Hermit Lake – Anderson et al., 2018) and to northern New Mexico (Chihuahueños Bog; Anderson et al., 2008b). However, increasing abundances in lower treeline thermophilous taxa, such as *Quercus*, *Juniperus*, and *Cercocarpus* and increases in *P. contorta*, and decreases in *Artemisia* (increase in P/A ratio; Fig. 5) indicate a rapid response to warming at that time. S/P ratios also show a decreasing trend, probably indicating a displacement of subalpine forest and *Picea* towards higher elevations at this time (Fig. 5). This change was probably a vegetation response to increasing summer insolation during the early Holocene (Laskar et al., 2004, Figs. 5–6). Sporadic fire activity is recorded during the early Holocene, but with peaks at ~8800 and 8400 cal yr BP, which could also point to the effects of higher than modern summer insolation and more forested vegetation in the area towards the end of this period.

The sedimentary record at Emerald Lake shows that lake levels were at their lowest during the early Holocene (Shuman et al., 2014, Fig. 6). Our multiproxy evidence provides additional support. For instance, low lacustrine algae occurrence, driven mostly by *Botryococcus* (Figs. 3 and 5) – a shallow water species (Guy-Ohlson, 1992; Batten and Grenfell, 1996) – suggest low lake levels, while hyperspectral values of the $RABD_{660}$ proxy suggests relatively high productivity (Fig. 6). These proxies were probably driven by elevated summer insolation, which warmed the shallow lake water and supported increased lake productivity. While few other studies have documented lowered lake levels in the central Rockies during this period, our results agree with a reconstruction of effective precipitation for San Luis Lake in southcentral Colorado, based on lake level and dust records (Yuan et al., 2013). Previous studies show that precipitation during the early Holocene was dominated by summer North American Monsoon (NAM) rains (Metcalfe et al., 2015, Fig. 6). However, even summer precipitation might have been low as it was not until ~8000 cal yr BP that the Bermuda High displaced north due to the melting of the Laurentide Ice Sheet

(Figs. 6 and 7), generating enhanced NAM summer precipitation (Metcalfe et al., 2015).

The observed warming trend in the early Holocene was interrupted, however, by a relatively cold and arid event centered at an age of ca. 8275 cal yr BP based on a minimum in thermophilous species such as *Quercus* or *Cercocarpus* and a significant drop in aquatic productivity (*Pediastrum* and *Botryococcus* algae and $RABD_{660}$ values), respectively (Figs. 5–7). This environmental change recorded in the Emerald Lake record could be the local expression of the well-known 8.2 ka cold event evidenced in the ice core records from central Greenland (Johnson et al., 2001; Rasmussen et al., 2007). The 8.2 ka event has been widely recognized throughout the northern hemisphere (Alley et al., 1997) and in previous pollen studies in the area (Cumbres Bog, Colorado; Johnson et al., 2013).

5.3. Mid-Holocene

Subalpine forest with *Picea*, *Abies* and *P. contorta* occurred around the lake area in the middle Holocene between 8200 and 4200 cal yr BP (zone EL-2; Fig. 3). We infer the forest type by comparing our pollen data with modern subalpine forest pollen samples from Colorado (Anderson et al., 2014), which also show percentages of *Picea* + *Abies* pollen around 15–35% and *Pinus* pollen of ca. 40%. Generally low AP/NAP ratios (Fig. 5) associated with this pollen zone may be consistent with sparse, open forest when the climate was drier than today. Evidence of low water levels are also consistent with this inference. Sediment cores taken in shallow water up to 34 m basinward from the modern Emerald Lake shoreline lack sediments from before ~5500 cal yr BP, likely requiring that lake levels were >3 m lower than today when pollen zone EL-2 accumulated in the lake center (Shuman et al., 2014). Increases in *Botryococcus* algal spores in the earliest part of the middle Holocene, with significant variability and maxima at ~8000 and 7000 cal yr BP, provide additional evidence of the low water but high productivity and further hydrologic variability before sediments began to accumulate in the near-shore areas of the modern lake (Fig. 5).

The pollen record is also consistent with higher than modern summer temperatures. Previous studies from the area show that upper treeline would have been between 80 and 300 m higher than today (Markgraf and Scott, 1981; Carrara et al., 1984, 1991; Fall 1997; Feiler et al., 1997; Anderson et al., 1999; Reasoner and Jodry, 2000; Toney and Anderson, 2006; Anderson et al., 2008a,b; Jiménez-Moreno et al., 2008, 2011; Briles et al., 2012; Jiménez-Moreno and Anderson, 2012a; Anderson et al., 2018). Here, we find that low elevation thermophilous species, such as *Quercus*, *Juniperus* and *Cercocarpus,* reached maximum abundances between 8000 and 6700 cal yr BP in subzone EL-2a. This pattern probably points to the occurrence of these species at their highest Holocene elevations at this time and thus adds to evidence for the highest regional temperatures in the middle Holocene, possibly >2 °C warmer than today (Andrews et al., 1975; Carrara et al., 1984; Elias, 1996). Maximum Holocene temperatures around 6800 cal yr BP agree with temperature reconstructions for the Central Rocky Mountains (Shuman, 2012) and the western North American region (Shuman and Marsicek, 2016) (Fig. 7).

These climate and vegetation changes occur in a period of generally high, but waning, summer insolation and its influence on summer temperatures (Kutzbach et al., 1998). Several authors (Kaufman et al., 2004; Renssen et al., 2009) have attributed this delay to the lingering effects of remnant continental ice, as the Laurentide Ice Sheet diminished in central North America (Fig. 7). Summer and autumn insolation anomalies continued through the middle Holocene (Berger, 1978; Kutzbach et al., 1998), and could have favored high temperatures and enhanced evaporation (Shuman et al., 2009), essentially "lengthening" the summer and "shortening" the winter temperature and precipitation seasons. Enhanced evaporation during warmest maxima could have triggered a drop in the Emerald Lake level (Shuman et al., 2014), increased erosion of inorganics into the lake (higher MS values) and minima in $RABD_{660}$ productivity values between 7000 and 6800 cal yr BP (Fig. 6). Contemporaneously, somewhat elevated CHAR values can be interpreted as greater fire activity during the warmest and driest conditions (Fig. 5).

Subalpine *Picea*, which started increasing at 7000 cal yr BP (boundary zones EL-2b-2c), reached its maximum at ca. 5700 cal yr BP, as reflected in the S/P ratio (Fig. 5). If so, *Picea* seems to have expanded downslope or locally in this area through the mid-Holocene when other evidence also indicates upslope movement of alpine treeline (Fall 1997). The combination of changes agrees with other alpine records from Colorado of Fall (1997) indicating a widening in both upper and lower boundaries of the *Picea-Abies* subalpine forest zone during the early-mid Holocene compared to today. The *Picea* peak at 5700 cal yr BP could also represent a phase of low temperatures, such as inferred for other areas of the mid-continent from ca. 6000-4800 cal yr BP (Shuman and Marsicek, 2016).

The *Picea* maxima at that time could also be explained by its preference for regions of abundant winter snow fall (Schrag et al., 2008), and combined with declining summer insolation in the middle and late Holocene, allowing for increased effective precipitation and soil humidity. Enhanced moisture availability may also explain why the *Picea* peak coincides with the apparent rise in Emerald Lake water levels at ca. 5700 cal yr BP (Fig. 6; Shuman et al., 2014). A deepening of the lake also agrees with the highest occurrences of *Nuphar*, probably pointing to an increase in the lakeshore area (Fig. 3). A change in the seasonality of precipitation in the area towards enhanced winter precipitation would produce an increase in effective precipitation and more runoff into the lake (Shuman et al., 2014). This is supported by $\delta^{18}O$ changes at San Luis Lake (Yuan et al., 2013; ca. 150 km to the south of Emerald Lake), interpreted as greater winter precipitation starting at 6700 cal yr BP and enhanced at ca. 5700 cal yr BP (Fig. 6). Numerous studies (Clement et al., 2000; Rein et al., 2005; Conroy et al., 2008) have shown enhanced modern-like ENSO variability after ca. 5500 cal yr BP which undoubtedly influenced winter precipitation variability here.

Further regional evidence supports the inferred increase in available moisture. In eastern New Mexico, dune stabilization began after ca. 5800 cal yr BP (Holliday, 1997), with at least periodic marsh and pond redevelopment after ca. 5500 cal yr BP (Holliday, 1989), indicating generally greater effective precipitation regionally (Wanner et al., 2008). These regional changes coincide with a rise in the water table in the Estancia Basin, New Mexico starting at ca. 5400 cal yr BP, which also points to an increase in winter precipitation in the area (Menking and Anderson, 2003). The striking covariation between the *Picea* record through the S/P and P/A ratios with other records that are proxies for NAM such as the $\delta^{18}O$ Buckeye Creek Cave speleothem record from west Virginia (Hardt et al., 2010) or the abundance in *Globigerinoides sacculifer* in the sedimentary record from the Gulf of Mexico (Poore et al., 2005) suggest a similar climatic cause-effect relationship (Fig. 8).

High percentages of *Picea* pollen and increasing lake levels at 5700 cal yr BP also coincide with a first increase in *P. edulis* between 6000 and 5300 cal yr BP at Emerald Lake (Fig. 6). Several previous regional pollen studies have noticed similar increases in *P. edulis*, mostly during the late middle and late Holocene, and suggested a relationship with a northward latitudinal migration of these species during the Holocene warming but also a possible response to

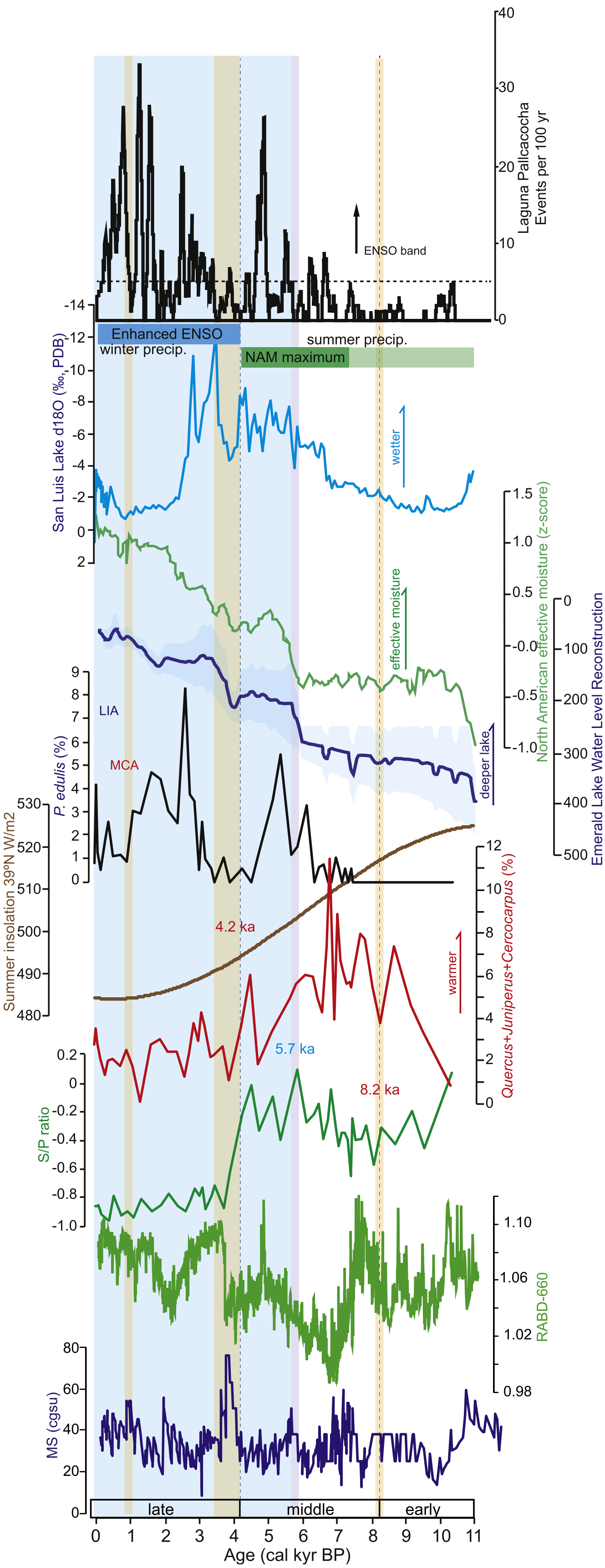

Fig. 6. Comparison of climatic proxies for effective precipitation with temperature from Emerald Lake (algae, pollen (S/P and A/P ratios, *Quercus* + *Juniperus* + *Cercocarpus* and *P. edulis*)), lake level variations from Emerald Lake (Shuman et al., 2014) and North American effective moisture (lake level and dust records) plotted as z-scores (Shuman and Marsicek, 2016), $\delta^{18}O$ of San Luis Lake, Colorado (note the inverted scale; Yuan et al., 2013), summer insolation (Laskar et al., 2004) and El Niño variability (Moy et al., 2002) for the last 11,000 cal yr BP. ENSO and North American Monsoon (NAM) dynamics are also shown after Metcalfe et al. (2015). Orange shadings represent arid periods-low effective precipitation and tentative correlations between the different proxies. Blue shading, starting at ca. 5700 cal yr BP, shows progressive increase in effective humidity, deepening of the Emerald and other lakes in North America and enhanced ENSO. MCA and LIA stand for Medieval Climate Anomaly and Little Ice Age, respectively. Red and blue color for 8.2, 5.7, 4.2 MCA and LIA means arid or humid periods, respectively.

increasing ENSO winter precipitation (Cole et al., 2008; Anderson and Feiler, 2009). Winter minimum precipitation is known to be significant in limiting modern *P. edulis* today (Cole et al., 2008). Other factors could include decreasing summer insolation and the increase in winter insolation leading to cooler summers and warmer winters during the middle-late Holocene (Holmgren et al., 2007), multidecadal climate variability and periodic drought (Jackson et al., 2005; Gray et al., 2006) or chance establishment by jay birds or Native Americans (Betancourt et al., 1991).

5.4. Late Holocene

The EL-2/EL-3 pollen zone boundary represents the most drastic vegetation change in the record at ca. 4200 cal yr BP, when *P. contorta* expanded at the expense of *Picea engelmannii*, and subsequently dominated the Emerald Lake area until present (Figs. 3 and 6). Currently, *P. contorta* predominates between ~2590 and 3050 m elevation, within the montane and subalpine vegetation belts, overlapping with *P. ponderosa* (ponderosa pine) and *Pseudotsuga menziesii* (Douglas-fir) at the low end of its elevation range and with *Picea* and *Abies* at its upper limits (Marr, 1967). *P. contorta* generally needs open canopy conditions for successful seed germination and is often tied to fire occurrence (Lotan and Critchfield, 1990). This tree-fire association exists because *P. contorta* cones are often adapted to wildfire, providing seeds that are viable for decades after fire, rapidly colonizing the area in full sunlight.

The sedimentary charcoal and *P. contorta* pollen data show a clear correspondence in the early Late Holocene (Fig. 4), where CHAR values reach their highest after ~3700 cal yr BP. However, enhanced fire activity follows the dramatic increase in *P. contorta* by ~500 years. The fact that this important vegetation change at 4200 cal yr BP happened during a period of minima in fire activity excludes fire as the main factor triggering this change. We suggest that, instead, rapidly changing climate could have triggered this significant environmental change. A widely documented mega-drought at ~4200 cal yr BP (Booth et al., 2005), which could be related with a minimum in ENSO winter precipitation (Fig. 6; Clement et al., 2000; Moy et al., 2002; Rein et al., 2005; Conroy et al., 2008), could be reflected in the Emerald Lake record by a minimum in algae (Fig. 6) and the low lake levels indicated by peak sand and MS in the cores (Fig. 4) (Shuman et al., 2014). While the ~4200 cal yr BP dry event has received a lot of attention globally (Thompson et al., 2002; Booth et al., 2005; Arz et al., 2006; Magny et al., 2009; Jiménez-Moreno and Anderson, 2012b), this would be the first documented occurrence of its effect in the southern Rocky Mountains.

These changes during the 4200-3700 cal yr BP interval are so dramatic, that we also advance three alternative explanations. (1) The change may have been facilitated by increasing winter insolation during the late Holocene, which would have allowed the upslope expansion of *Picea* due to warming winter temperatures (Fig. 6). (2) It might be due to increasing winter insolation in the late Holocene and the change in precipitation patterns at this time

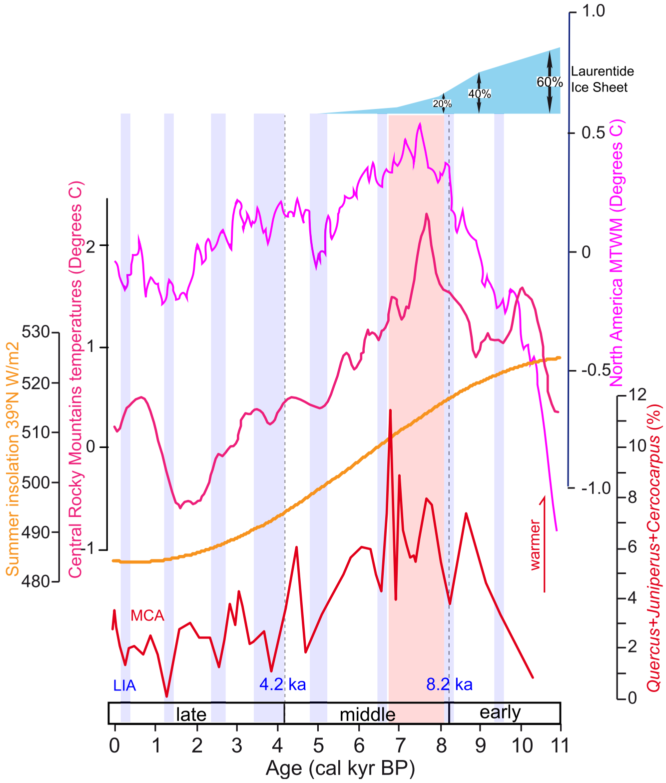

Fig. 7. Comparison of paleotemperatures deduced from Emerald Lake and reconstructions from the Rocky Mountains (Shuman, 2012) and North America (Shuman and Marsicek, 2016; MTMW stands for mean temperature of the warmest month), summer insolation at 39° N latitude (Laskar et al., 2004) and area of the Laurentide ice sheet as a fraction of the area during the last glacial maximum (from Shuman et al., 2009). Red shading highlights the warmest temperatures recorded at Emerald Lake and North America. Blue shadings point to possible correlations between cooling events in all the records. 8.2, 4.2, MCA and LIA are well-known global climatic events. MCA and LIA stand for Medieval Climate Anomaly and Little Ice Age, respectively.

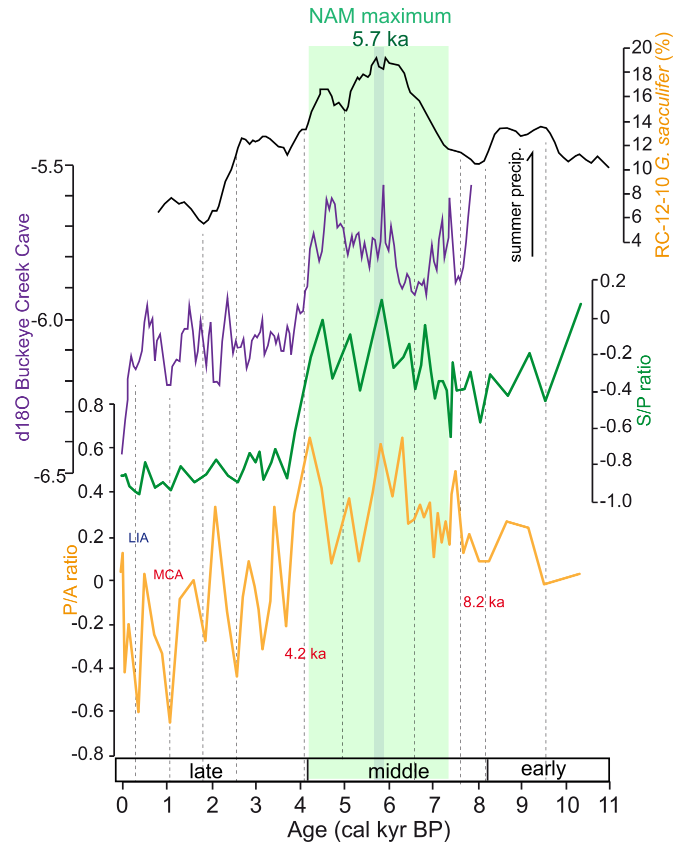

Fig. 8. Comparison of paleoclimate pollen proxies from Emerald Lake (P/A and S/P ratios) with other proxies recording NAM precipitation: $\delta^{18}O$ from the Buckeye Creek Cave speleothem record from West Virginia (Hardt et al., 2010) and abundance in *Globigerinoides sacculifer* in the sedimentary record from the Gulf of Mexico (Poore et al., 2005). Green shading shows maxima in NAM precipitation deduced by this comparison and blue shading at around 5700 cal yr BP points to NAM maxima. Dashed lines show possible correlations between the records. Note the covariation between the $\delta^{18}O$ speleothem record from West Virginia and S/P ratios. 8.2, 4.2, MCA and LIA are well-known climatic events discussed in the text.

with the transition from summer-dominated NAM to winter-dominated precipitation (e.g., ENSO; Figs. 6 and 8). Because summer precipitation may be readily evapotranspiration, a seasonal shift in precipitation could enhance total effective moisture in soils while deep winter snow could insulate soils and young trees from freezing temperatures. Consistent with an increase in effective moisture, Emerald Lake also did not reach near modern lake levels until after a period of low water between ca. 4200-3400 cal yr BP based on the initial accumulation of lake muds in a core located 25 m from shore (Figs. 4 and 6; Shuman et al., 2014). Potentially, the EL-2/EL-3 pollen zone boundary relates to vegetation changes that required these maximum water levels. (3) The vegetation changes could be related to changes in cold air drainage and an increase in minimum temperatures in the Halfmoon Creek valley where Emerald Lake is located. If minimum temperatures increased throughout the Holocene in response to increased atmospheric carbon dioxide and winter insolation as simulated in climate model experiment (e.g., Alder and Hostetler, 2015), then pine seedling mortality and related ecological effects of extreme cold may have been reduced allowing for the replacement of spruce-fir forests of the early- and mid-Holocene with *P. contorta* forests and *P. edulis* woodlands after ~4200 cal yr BP (Fig. 5). The sharp reduction in *Quercus* pollen percentages at the same time may be consistent with reduced summer temperatures at this time even if minimum temperatures increased, but such a change in temperature seasonality would be consistent with seasonal insolation forcing (Laskar et al., 2004; Alder and Hostetler, 2015). It is possible that no one factor can account for such a dramatic change in vegetation, and that this transition was facilitated by a combination of influences, but it illustrates the potential for dramatic ecosystem state changes in the context of climate change.

The Emerald Lake charcoal record shows significant variability during the Late Holocene and high fire activity is recorded with peaks at ca. 3770, 2500, 1000–900 and 200-80 cal yr BP, coinciding with peaks in *P. contorta* and minima in S/P ratios, further confirming the *P. contorta*-fire association. The late Holocene is known to be a period of considerable variability in effective precipitation within the region, typified by periodic decadal-scale droughts alternating with extended wetter periods (Cook et al., 2004; MacDonald, 2007; Meko et al., 2007). Periodic droughts impacting high-elevation forests, stocked with considerable biomass, led to higher fire activity during those above mentioned periods of the late Holocene (Anderson et al., 2008a, b).

A significant increase in *P. edulis* pollen percentages, recording a maximum occurrence at ~2570 cal yr BP, and higher lake levels between ~3500 and 1000 cal yr BP (Shuman et al., 2014), further indicate the importance of enhanced winter precipitation, perhaps ENSO, in the late-Holocene. Maxima in lake levels between 3500 and 2500 are also recorded in the San Luis lake in Colorado (Yuan et al., 2013, Fig. 6). The increase in *P. edulis* around this time is a widespread phenomenon in Colorado and New Mexico (Anderson

and Feiler, 2009; Jiménez-Moreno et al., 2011; Jiménez-Moreno and Anderson, 2012a; Anderson et al., 2018). At Emerald Lake, the covariation between lake level changes and *P. edulis* since its first occurrences in the area (Fig. 6) may indicate a cause/effect relationship. One of the primary regions of *P. edulis* distribution in the area is south-western Colorado (Cole et al., 2008), and because prevailing winds often derive from the southwest at Emerald Lake, the atmospheric pollen load there may represent the regional expansion of the species.

A continuous cooling trend over the last few millennia is also recorded at Emerald Lake by a progressive decline in the pollen percentages of *Quercus* and other thermophilous species such as *Juniperus* and *Cercocarpus* (Fig. 7). These species probably retreated to lower elevations under colder conditions. Decreasing summer insolation in the late Holocene (Neoglacial) led to cooler summers than earlier in the Holocene (Laskar et al., 2004; Alder and Hostetler, 2015), and most likely caused these vegetation trends. However, a warm and dry event, characterized in the Emerald Lake record by a peak in thermophilous taxa such as *Quercus*, *Juniperus* and *Cercocarpus* and a minimum in S/P ratios, low *Pediastrum*, and a peak in fire activity, occurred at around 1000 cal yr BP in the Emerald Lake record, which could be related to general warm and arid conditions, with abundant fires in the area during the Medieval Climate Anomaly (MCA) between 1200 and 850 cal yr BP (Calder et al., 2015) and high aeolian activity associated with drought (Miao et al., 2007). This event might have been associated with centennial-scale low ENSO activity and cooler tropical Pacific sea surface temperatures and persistent La Niña type conditions interpreted for this time (i.e., Moy et al., 2002; Metcalfe et al., 2015, Fig. 6).

6. Conclusions

Multiproxy data clearly document that environments around and within Emerald Lake, Colorado have been highly sensitive to changes in climate since the beginning of the Holocene. The comparison of the pollen and sedimentation with the lake-level record of Emerald Lake indicate:

1. Climate warming in the early and middle Holocene related with increase in summer insolation. Low lake levels occurred at that time, pointing to low winter precipitation.
2. Maxima in temperatures are reached at ca. 6800 cal yr BP, recorded by the highest elevation of lower treeline.
3. A first substantial decrease in temperatures and an increase in winter precipitation, perhaps triggered by reduced summer insolation and enhanced ENSO, is recorded in both pollen and lake levels at ca. 5700 cal yr BP.
4. *P. contorta* boosted and completely occupied the area at ca. 4200 cal yr BP until present, probably due to a combination of insolation changes and a significant cold and arid event during a change in precipitation patterns with the weakening of North American Monsoon (NAM) and stronger winter precipitation dynamics.
5. Winter precipitations seem to be highest between 3000 and 1000 cal yr BP, possibly due to enhanced ENSO variability in the late-Holocene.
6. A continuous cooling trend is also recorded in the Emerald Lake record in the late Holocene.
7. Arid events are recorded at 8200, 4200 and 1000 cal yr BP and could be related with well-known global arid events and low ENSO activities.

Acknowledgements

Support for the present study derives from the US Geological Survey's Western Mountain Initiative Cooperative Agreement No. 99CRAG0019 to RSA; project P11-RNM 7332 funded by Consejería de Economía, Innovacion, Ciencia y Empleo de la Junta de Andalucia; the projects CGL2013-47038-R and CGL2017-85415-R funded by Ministerio de Economía y Competitividad of Spain and Fondo Europeo de Desarrollo Regional FEDER; and the research group RNM-190 (Junta de Andalucía) (all to GJM). We thank Craig Allen (USGS) for his unwavering support of our research; Amy Martin and Taylor Joyal for helping with the Emerald Lake fieldwork; Doug Hammond (USC) for determining the ^{210}Pb ages of Emerald EL-07-01 core; and Nick McKay (NAU) for the use of his hyperspectral camera.

Appendix A. Supplementary data

Supplementary data to this article can be found online at https://doi.org/10.1016/j.quascirev.2019.03.013.

References

Alder, J.R., Hostetler, S.W., 2015. Global climate simulations at 3000-year intervals for the last 21 000 years with the GENMOM coupled atmosphere-ocean model. Clim. Past 11 (3), 449–471.
Alley, R.B., Mayewski, P.A., Sowers, T., Stuiver, M., Taylor, K.C., Clark, P.U., 1997. Holocene climatic instability: a prominent, widespread event 8200 yr ago. Geology 25, 483–486.
Anderson, L., 2012. Rocky mountain hydroclimate: Holocene variability and the role of insolation, ENSO, and the north American monsoon. Glob. Planet. Chang. 92–93, 198–208.
Anderson, R.S., Feiler, E., 2009. Holocene vegetation and climate change on the Colorado Great Plains, USA, and the invasion of Colorado piñon (*Pinus edulis*). J. Biogeogr. 36, 2279–2289.
Anderson, R.S., Hasbargen, J., Koehler, P.A., Feiler, E.J., 1999. Late Wisconsin and Holocene subalpine forests of the markagunt plateau of Utah, southwestern Colorado plateau. USA Arctic Antarctic Alpine Res. 31 (4), 366–378.
Anderson, R.S., Allen, C.D., Toney, J.L., Jass, R.B., Bair, A.N., 2008a. Holocene vegetation and fire regimes in subalpine and mixed conifer forests, southern Rocky Mountains, Colorado. Int. J. Wildland Fire 17, 96–114.
Anderson, R.S., Jiménez-Moreno, G., Ager, T., Porinchu, D., 2014. High-elevation paleoenvironmental change during MIS 4 – 6 in the central Rockies of Colorado as determined from pollen analysis. Quat. Res. 82, 542–552.
Anderson, R.S., Jass, R.B., Toney, J.L., Allen, C.D., Cisneros-Dozal, L.M., Hess, M., Heikoop, J., Fessenden, J., 2008b. Development of the mixed conifer forest in northern New Mexico and its relationship to Holocene environmental change. Quat. Res. 69, 263–275.
Anderson, R.S., Soltow, H.R., Jiménez-Moreno, G., 2018. Postglacial environmental change of a high elevation forest near Hermit Lake, Sangre de Cristo Range of south central Colorado. In: Starratt, S.W., Rosen, M.R. (Eds.), Chapter 13, "From Saline to Freshwater: the Diversity of Western Lakes in Space and Time", vol. 536. Geological Society of America Special Paper, pp. 1–XXX.
Andrews, J.T., Carrara, P.E., King, F.B., Stuckenrath, R., 1975. Holocene environmental changes in the alpine zone, northern San Juan Mountains, Colorado: evidence from bog stratigraphy and palynology. Quat. Res. 5, 173–197.
Antinao, J.L., McDonald, E., 2013. An enhanced role for the Tropical Pacific on the humid Pleistocene-Holocene transition in southwestern North America. Quat. Sci. Rev. 78, 319–341.
Arz, H.W., Lamy, F., Pätzold, J., 2006. A pronounced dry event recorded around 4.2 ka in brine sediments from the northern Red Sea. Quat. Res. 66, 432–441.
Benson, L., Madole, R., Landis, G., Gosse, J., 2005. New data for Pleistocene Pinedale alpine glaciation from southwestern Colorado. Quat. Sci. Rev. 24, 49–65.
Barron, J.A., Anderson, L., 2011. Enhanced late Holocene ENSO/PDO expression along the margins of the eastern North Pacific. Quat. Int. 235, 3–12.
Batten, D.J., Grenfell, H.R., 1996. Botryococcus. In: Jansonius, J., McGregor, D.C. (Eds.), Palynology: Principles and Applications, vol. 1. American Association of Stratigraphic Palynologists Foundation, pp. 205–214.
Berger, A., 1978. Long-term variations of daily insolation and Quaternary climatic changes. J. Atmos. Sci. 35, 2362–2367.
Betancourt, J.L., Schuster, W.S., Mitton, J.B., Anderson, R.S., 1991. Fossil and genetic history of a pinyon pine (*Pinus edulis*) isolate. Ecology 72, 1685–1697.
Booth, R.K., Jackson, S.T., Forman, S.L., Kutzbach, J.E., Bettis III, E.A., Kreigs, J., Wright, D.K., 2005. A severe centennial-scale drought in midcontinental North America 4200 years ago and apparent global linkages. Holocene 15, 321–328.
Blaauw, M., 2010. Methods and code for 'classical' age-modelling of radiocarbon sequences. Quat. Geochronol. 5, 512–518.
Briles, C.E., Whitlock, C., Meltzer, D.J., 2012. Last glacial-interglacial environments in

the southern Rocky Mountains, USA and implications for Younger Dryas-age human occupation. Quat. Res. 77, 96–103.
Butz, C., Grosjean, M., Fischer, D., Wunderle, S., Tylmann, W., Rein, B., 2015. Hyperspectral imaging spectroscopy: a promising method for the biogeochemical analysis of lake sediments. J. Appl. Remote Sens. 9, 1–20.
Cairns, D.M., Malanson, G.P., 1998. Environmental variables influencing the carbon balance at the alpine treeline: a modeling approach. J. Veg. Sci. 9, 679–692.
Calder, J., Stopka, C., Parker, D., Jiménez-Moreno, G., Shuman, B.N., 2015. Medieval warming initiated exceptionally large wildfire outbreaks in the rocky mountains. Proc. Natl. Acad. Sci. Unit. States Am. 112, 13261–13266.
Carrara, P.E., Mode, W.N., Rubin, M., Robinson, S.W., 1984. Deglaciation and postglacial timberline in the san juan mountains, Colorado. Quat. Res. 21, 42–55.
Carrara, P.E., Trimble, D.A., Rubin, M., 1991. Holocene tree line fluctuations in the northern San Juan Mountains, Colorado, U.S.A., as indicated by radiocarbon-dated conifer wood. Arct. Alp. Res. 23, 233–246.
Carter, V., Lundeen, Z., Brunelle, A., Shinker, J., Bartlein, P., Koll, R., Petersen, K., Power, M., Morris, J., Anderson, R.S., Turney, L., 2017. A 1,500-year synthesis of wildfire activity stratified by elevation from the U.S. Rocky Mountains. Quat. Int. 488, 107–119.
Clement, A.C., Seager, R., Cane, M.A., 2000. Suppression of El Niño during the mid-Holocene by changes in the Earth's orbit. Paleoceanography 15, 731–741.
Cole, K.L., Fisher, J., Arundel, S.T., Cannella, J., Swift, S., 2008. Geographical and climatic limits of needle types of one- and two-needled pinyon pines. J. Biogeogr. 35, 257–269.
Conroy, J.L., Overpeck, J.T., Cole, J.E., Shanahan, T.M., Steinitz-Kannan, M., 2008. Holocene changes in eastern tropical Pacific climate inferred from a Galápagos lake sediment record. Quat. Sci. Rev. 27 (11–12), 1166–1180.
Cook, E.R., Woodhouse, C.A., Eakin, C.M., Meko, D.M., Stahle, D.W., 2004. Long-term aridity changes in the western United States. Science 306, 1015–1018.
Cook, B.I., Ault, T.R., Smerdon, J.E., 2015. Unprecedented 21st century drought risk in the American southwest and central plains. Sci. Adv. 1, e1400082.
Coop, J.D., Givnish, T.J., 2008. Constraints on tree seedling establishment in montane grasslands of the Valles Caldera, New Mexico. Ecology 89 (4), 1101–1111.
Das, B., Vinebrooke, R.D., Sanchez-Azofeifa, A., et al., 2005. Inferring sedimentary chlorophyll concentrations with reflectance spectroscopy: a novel approach to reconstructing historical changes in the trophic status of mountain lakes. Can. J. Fish. Aquat. Sci. 62, 1067–1078.
Dennison, P.E., Brewer, S.C., Arnold, J.D., Moritz, M.A., 2014. Large wildfire trends in the western United States, 1984-2011. Geophys. Res. Lett. 41, 1–6.
Donders, T.H., Wagner-Cremer, F., Visscher, H., 2008. Integration of proxy data and model scenarios for the mid- Holocene onset of modern ENSO variability. Quat. Sci. Rev. 27, 571–579.
Elias, S.A., 1996. Late Pleistocene and Holocene seasonal temperatures reconstructed from fossil beetle assemblages in the Rocky Mountains. Quat. Res. 46, 311–318.
Faegri, K., Iversen, J., 1989. Textbook of Pollen Analysis: Caldwell. Blackburn Press, New Jersey, pp. 69–90.
Fall, P.L., 1997. Timberline fluctuations and late Quaternary paleoclimates in the southern Rocky Mountains, Colorado. Geol. Soc. Am. Bull. 109, 1306–1320.
Feiler, E.J., Anderson, R.S., Koehler, P.A., 1997. Late Quaternary paleoenvironments of the White River Plateau, Colorado, U.S.A. Arctic and Alpine Research, 29, pp. 53–62.
Gray, S.T., Betancourt, J.L., Jackson, S.T., et al., 2006. Role of multidecadal climate variability in a range extension of pinyon pine. Ecology 87, 1124–1130.
Grimm, E.C., 1987. CONISS: A FORTRAN 77 program for stratigraphically constrained cluster analysis by the method of incremental sum of squares. Comput. Geosci. 13, 13–35.
Grosjean, M., Amann, B., Butz, C., Rein, B., Tylmann, W., 2014. Hyperspectral imaging: a novel, non-destructive method for investigating sub-annual sediment structures and composition. Pages Mag. 22 (1), 10–11.
Guido, Z.S., Ward, D.J., Anderson, R.S., 2007. Pacing the post–last glacial maximum demise of the animas valley glacier and the san juan mountain ice cap, Colorado. Geology 35, 739–742.
Guy-Ohlson, D., 1992. Botryococcus as an aid in the interpretation of palaeoenvironment and depositional processes. Rev. Palaeobot. Palynol. 71, 1–15.
Hardt, B., Rowe, H.D., Springer, G.S., Cheng, H., Edwards, R.L., 2010. The seasonality of east central North American precipitation based on three coeval Holocene speleothems from southern West Virginia. Earth Planet. Sci. Lett. 295, 342–348.
Haug, G.H., Hughen, K.A., Sigman, D.M., Peterson, L.C., Röhl, U., 2001. Southward migration of the Intertropical Convergence Zone through the Holocene. Science 293, 1304–1308.
Higuera, P.E., Briles, C.E., Whitlock, C., 2014. Fire-regime complacency and centennial through millennial-scale climate change in Rocky Mountain subalpine forests, Colorado, USA. J. Ecol. 102, 1429–1441.
Holliday, V.T., 1989. The blackwater draw formation (Quaternary): A 1.4-plus m.y. record of eolian sedimentation and soil formation on the Southern High Plains. Geol. Soc. Am. Bull. 101, 1598–1607.
Holliday, V.T., 1997. Origin and evolution of lunettes on the High Plains of Texas and New Mexico. Quat. Res. 47, 54–69.
Holmgren, C.A., Norris, J., Betancourt, J.L., 2007. Inferences about Winter temperatures and summer rains from the late Quaternary record of C4 perennial grasses and C3 desert shrubs in the northern Chihuahuan Desert. J. Quat. Sci. 22, 141–161.
Jackson, S.T., Betancourt, J.L., Lyford, M.E., Gray, S.T., Rylander, K.A., 2005. A 40,000 year woodrat-midden record of vegetational and biogeographic dynamics in northeastern Utah. J. Biogeogr. 32, 1085–1106.
Jacobs, B.F., 1985. Identification of pine pollen from the southwestern United States. Am. Assoc. Stratigr. Palynol. Contrib. Ser. 16, 155–168.
Jiménez-Moreno, G., Anderson, R.S., 2012a. Pollen and macrofossil evidence of Late Pleistocene and Holocene treeline fluctuations from an alpine lake in Colorado, USA. Holocene 23, 68–77.
Jiménez-Moreno, G., Anderson, R.S., 2012b. Holocene vegetation and climate change recorded in alpine bog sediments from the Borreguiles de la Virgen, Sierra Nevada, southern Spain. Quat. Res. 77, 44–53.
Jiménez-Moreno, G., Fawcett, P.J., Anderson, R.S., 2008. Millennial- and centennial scale vegetation and climate changes during the late Pleistocene and Holocene from northern New Mexico (USA). Quat. Sci. Rev. 27, 1442–1452.
Jiménez-Moreno, G., Anderson, R.S., Atudorei, V., Toney, J.L., 2011. A high-resolution record of climate, vegetation, and fire in the mixed conifer forest of northern Colorado, USA. Geol. Soc. Am. Bull. 123, 240–254.
Johnson, S.J., Dahl-Jensen, D., Gundestrup, N., Steffensen, J.P., Clausen, H.B., Miller, H., Masson-Delmotte, V., Sveinbjornsdottir, A.E., White, J., 2001. Oxygen isotope and palaeotemperature records from six Greenland ice-core stations: Camp Century, DYE-3, GRIP, GISP2, Renland, and NorthGRIP. J. Quat. Sci. 16, 299–307.
Johnson, B.G., Jiménez-Moreno, G., Eppes, M.C., Diemer, J.A., Stone, J.R., 2013. A multiproxy record of postglacial climate variability from a shallowing, 12-m deep sub-alpine bog in the southeastern San Juan Mountains of Colorado, USA. Holocene 23, 1028–1038.
Jolly, W.M., Cochrane, M.A., Freeborn, P.H., Holden, Z.A., Brown, T.J., Williamson, G.J., Bowman, D.M., 2015. Climate-induced variations in global wildfire danger from 1979 to 2013. Nat. Commun. 6, 7537.
Kaufman, D.S., Ager, T.A., Anderson, N.J., Andrews, J.T., Bartlein, P.J., Brubaker, L.B., Coats, L.L., Cwynar, L.C., Duvall, M.L., Dyke, A.S., Edwards, M.E., Eisner, W.R., Gajewski, K., Geirsdóttir, A., Hu, F.S., Jennings, A.E., Kaplan, M.R., Kerwin, M.W., Lozhkin, A.V., MacDonald, G.M., Miller, G.H., Mock, C.J., Oswald, W.W., Otto-Bliesner, B.L., Porinchu, D.F., Rühland, K., Smol, J.P., Steig, E.J., Wolfe, B.B., 2004. Holocene thermal maximum in the western Arctic (0–180ºW). Quat. Sci. Rev. 23, 529–560.
Kutzbach, J., Gallimore, R., Harrison, S., Behling, P., Selin, R., Laarif, F., 1998. Climate and biome simulations for the past 21,000 years. Quat. Sci. Rev. 17, 473–506.
Lagenheim, J.H., 1962. Vegetation and environmental patterns in the Crested Butte area, Gunnison County, Colorado. Ecol. Monogr. 32 (3), 249–285.
Laskar, J., Robutel, P., Joutel, F., Gastineau, M., Correia, A.C.M., Levrard, B., 2004. A long term numerical solution for the insolation quantities of the earth. Astron. Astrophys. 428, 261–285.
Leatherman, D.A., 2008. Report on the Health of Colorado's Forests. Colorado State Forest Service, Denver, CO.
Legg, T.E., Baker, R.G., 1980. Palynology of Pinedale sediments, Devlins Park, Boulder County, Colorado. Arct. Alp. Res. 12 (3), 319–333.
Lotan, J.E., Critchfield, W.B., 1990. *Pinus contorta* (Dougl. ex. Loud.) lodgepole pine. In: Burns, R.M., Honkala, B.H. (Eds.), Technical Coordinators. Silvics of North America, vol. 1. Conifers. USDA Agricultural Handbook 654, Washington, DC, USA, pp. 302–315.
MacDonald, G.M., 2007. Severe and sustained drought in southern California and the West: Present conditions and insights from the past on causes and impacts. Quat. Int. 173–174, 87–100.
Magny, M., Vannière, B., Zanchetta, G., Fouache, E., Touchais, G., Petrika, L., Coussot, C., Arnaud, F., 2009. Possible complexity of the climatic event around 4300- 3800 cal. BP in the central and western Mediterranean. Holocene 19, 823–833.
Maher, L.J., 1963. Pollen analyses of surface materials from the southern San Juan Mountains, Colorado. Geol. Soc. Am. Bull. 74, 1485–1504.
Markgraf, V., Scott, L., 1981. Lower timberline in central Colorado during the past 15,000 yr. Geology 9, 231–234.
Marr, J.W., 1967. Ecosystems of the East Slope of the Front Range in Colorado. University of Colorado Studies, Series in Biology, vol. 8. University of Colorado Press, Boulder.
Mathys, A.S., Coops, N.C., Waring, R.H., 2017. A ecoregion assessment of projected tree species vulnerabilities in western North America through the 21st century. Glob. Chang. Biol. 23, 920–932.
McDowell, N.G., Allen, C.D., 2015. Darcy's law predicts widespread forest mortality under climate warming. Nat Clim Chang Nature Research, 5, pp. 669–672.
Meko, D.M., Woodhouse, C.A., Baisan, C.A., Knight, T., Lukas, J.J., Hughes, M.K., Salzer, M.W., 2007. Medieval drought in the upper Colorado River Basin. Geophys. Res. Lett. 34, L10705.
Menking, K.M., Anderson, R.Y., 2003. Contributions of La Niña and El Niño to middle Holocene drought and late Holocene moisture in the American southwest. Geology 31, 937–940.
Menking, K.M., Polyak, V.J., Anderson, R.Y., Asmerom, Y., 2018. Climate history of the southwestern United States based on Estancia Basin hydrologic variability from 69 to 10 ka. Quat. Sci. Rev. 200, 237–252.
Metcalfe, S.E., Barron, J.A., Davies, S.J., 2015. The Holocene history of the North American Monsoon: 'known knowns' and 'known unknowns' in understanding its spatial and temporal complexity. Quat. Sci. Rev. 120, 1–27.
Miao, X.D., Mason, J.A., Swinehart, J.B., Loope, D.B., Hanson, P.R., Goble, R.J., Lui, X.D., 2007. A 10,000 year record of dune activity, dust storms, and severe drought in the central Great Plains. Geology 35, 119–122.
Michelutti, N., Smol, J.P., 2016. Visible spectroscopy reliably tracks trends in paleo-production. J. Paleolimnol. 56 (4), 253–265.

Moritz, M.A., Parisien, M.-A., Batllori, E., Krawchuk, M.A., Van Dorn, J., Ganz, D.J., Hayhoe, K., 2012. Climate change and disruptions to global fire activity. Ecosphere 3 (6), 49.
Moy, C.M., Seltzer, G.O., Rodbell, D.T., Anderson, D.M., 2002. Variability of El Niño/Southern Oscillation activity at millennial timescales during the Holocene epoch. Nature 420, 162–165.
Neilson, R.P., Wullstein, L.H., 1983. Biogeography of two southwest American oaks in relation to atmospheric dynamics. J. Biogeogr. 10 (4), 275–297.
Nelson, A.R., Shroba, R.R., 1998. Soil relative dating of moraine and outwash-terrace sequences in the northern part of the Upper Arkansas Valley, Central Colorado, U.S.A. Arct. Alp. Res. 30 (4), 349–363.
Parnell, A.C., Haslett, J., Allen, J.R.M., Buck, C.E., Huntley, B., 2008. A flexible approach to assessing synchroneity of past events using Bayesian reconstructions of sedimentation history. Quat. Sci. Rev. 27, 1872–1885.
Polyak, Victor J., Asmerom, Y., Burns, S.J., Lachniet, M.S., 2012. Climatic backdrop to the terminal Pleistocene extinction of North American mammals. Geology 40 (11), 1023–1026.
Poore, R.Z., Pavich, M.J., Grissino-Mayer, H.D., 2005. Record of the North American southwest monsoon from Gulf of Mexico sediment cores. Geology 33, 209–212.
Power, M.J., Marlon, J., Ortiz, N., Bartlein, P.J., Harrison, S.P., Mayle, F.E., et al., 2008. Changes in fire regime since the Last Glacial Maximum: An assessment based on a global synthesis and analysis of charcoal data. Clim. Dyn. 30 (7–8), 887–907.
Rasmussen, S.O., Vinther, B.M., Clausen, H.B., Anderson, K.K., 2007. Early Holocene climate oscillations recorded in three Greenland ice cores. Quat. Sci. Rev. 26, 1907–1914.
Reasoner, M.A., Jodry, M.A., 2000. Rapid response of alpine timberline vegetation to the Younger Dryas climate oscillation in the Colorado Rocky Mountains, USA. Geology 28, 51–54.
Rein, B., Sirocko, F., 2002. In-situ reflectance spectroscopy - Analysing techniques for high-resolution pigment logging in sediment cores. Int. J. Earth Sci. 91 (5), 950–954.
Reimer, P.J., Bard, E., Bayliss, A., Beck, J.W., Blackwell, P.G., Bronk Ramsey, C., Buck, C.E., Cheng, H., Edwards, R.L., Friedrich, M., Grootes, P.M., Guilderson, T.P., Haflidason, H., Hajdas, I., Hatté, C., Heaton, T.J., Hoffmann, D.L., Hogg, A.G., Hughen, K.A., Kaiser, K.F., Kromer, B., Manning, S.W., Niu, M., Reimer, R.W., Richards, D.A., Scott, E.M., Southon, J.R., Staff, R.A., Turney, C.S.M., van der Plicht, J., 2013. IntCal13 and Marine13 radiocarbon age calibration curves 0–50,000 years cal BP. Radiocarbon 55 (4), 1869–1887.
Rein, B., Luckge, A., Reinhardt, L., Sirocko, F., Wolf, A., Dullo, W.C., 2005. El Niño variability off Peru during the last 20,000 years. Paleoceanography 20 (4), PA4003.
Renssen, H., Seppa, H., Heiri, O., et al., 2009. The spatial and temporal complexity of the Holocene thermal maximum. Nat. Geosci. 2, 411–414.
Romme, W.H., Clement, J., Hicke, J.A., Kulakowski, D., MacDonald, L.H., Schoennagel, T., Veblen, T.T., 2006. Recent Forest Insect Outbreaks and Fire Risk in Colorado Forests: A Brief Synthesis of Relevant Research. Colorado Forest Restoration Institute, Colorado State University, Fort Collins. www.cfri.colostate.edu/docs/cfri_insect.pdf.
Scheer, H., 2006. An overview of chlorophylls and bacteriochlorophylls: biochemistry, biophysics, functions and applications. In: Grimm, B., Porra, R., Rudiger, W., Scheer, H. (Eds.), Chlorophylls and Bacteriochlorophylls. Springer, Dordrecht, pp. 1–26.
Schrag, A.M., Bunn, A.G., Graumlich, L.J., 2008. Influence of bioclimatic variables on treeline conifer distribution in the Greater Yellowstone Ecosystem: implications for species of conservation concern. J. Biogeogr. 35, 698–710.
Schweinsberg, A.D., Briner, J.P., Shroba, R.R., Licciardi, J.M., Leonard, E.M., Brugger, K.A., Russell, C.M., 2016. Pinedale glacial history of the upper Arkansas River valley: New moraine chronologies, modeling results, and geologic mapping. In: Keller, S.M., Morgan, M.L. (Eds.), Unfolding the Geology of the West, vol. 44. Geological Society of America Field Guide, pp. 335–353.
Shuman, B., 2012. Recent Wyoming temperature trends, their drivers, and impacts in a 14,000-year context. Clim. Change 112 (2), 429–447.
Shuman, B.N., Marsicek, J., 2016. The structure of Holocene climate change in mid-latitude North America. Quat. Sci. Rev. 141, 38–51.
Shuman, B.N., Serravezza, M., 2017. Patterns of hydroclimatic change in the Rocky Mountains and surrounding regions since the last glacial maximum. Quat. Sci. Rev. 173, 58–77.
Shuman, B., Henderson, A.K., Colman, S.M., Stone, J.R., Fritz, S.C., Stevens, L.R., Power, M.J., Whitlock, C., 2009. Holocene lake-level trends in the Rocky Mountains, U.S.A. Quat. Sci. Rev. 28, 1861–1879.
Shuman, B.N., Carter, G.E., Hougardy, D.D., Powers, K., Shinker, J.J., 2014. A north-south moisture dipole at multi-century scales in the Central and Southern Rocky Mountains, U.S.A., during the late Holocene. Rocky Mt. Geol. 49, 33–49.
Snowball, I., Sandgren, P., 2001. Application of Mineral Magnetic Techniques to Paleolimnology. Tracking Environmental Change Using Lake Sediments 2. Kluwer Academic Publishers, Dordrecht.
Stuiver, M., Reimer, P.J., 1993. Extended 14C data base and revised CALIB 3.0 14C age calibration program. Radiocarbon 35, 215–230.
Sturrock, R.N., Frankel, S.J., Brown, A.V., Hennon, P.E., Kliejunas, J.T., Lewis, K.J., et al., 2011. Climate change and forest diseases. Plant Pathol. (Oxf.) 60, 133–149.
Thompson, L.G., Mosley-Thompson, E., Davis, M.E., Henderson, K.A., Brecher, H.H., Zagorodnov, V.S., Mashiotta, T.A., Lin, P.N., Mikhalenko, V.N., Hardy, D.R., Beer, J., 2002. Kilimanjaro ice core records: evidence of Holocene climate change in tropical Africa. Science 298, 589–593.
Toney, J.L., Anderson, R.S., 2006. A postglacial paleoecological record from the San Juan Mountains of Colorado USA: fire, climate and vegetation history. Holocene 16, 505–517.
Trachsel, M., Grosjean, M., Schnyder, D., Kamenik, C., Rein, B., 2010. Scanning reflectance spectroscopy (380-730 nm): a novel method for quantitative high-resolution climate reconstructions from minerogenic lake sediments. J. Paleolimnol. 44, 979–994.
Tweto, O., Moench, R.H., Reed Jr., J.C., 1978. Geologic Map of the Leadville 1 Degree X 2 Degrees Quadrangle, Northwestern Colorado, U.S. Geological Survey Miscellaneous Investigations Series Map I-999, Scale 1:250,000, 1 Sheet.
von Gunten, L., Grosjean, M., Rein, B., Urrutia, R., Appleby, P., 2009. A quantitative high-resolution summer temperature reconstruction based on sedimentary pigments from Laguna Aculeo, central Chile, back to AD 850. Holocene 19, 873–881.
Walker, M.J., Berkelhammer, M., Björck, S., Cwynar, L.C., Fisher, D.A., Long, A.J., Lowe, J.J., Newnham, R.M., Rasmussen, S.O., Weiss, H., 2012. Formal subdivision of the Holocene series/epoch: a discussion paper by a working group of INTIMATE (integration of ice-core, marine and terrestrial records) and the subcommission on quaternary stratigraphy (international commission on stratigraphy). J. Quat. Sci. 27, 649–659.
Wanner, H., Beer, J., Butikofer, J., Crowley, T.J., Cubasch, U., Fluckiger, J., Goosse, H., Grosjean, M., Joos, F., Kaplan, J.O., Kuttel, M., Muller, S.A., Prentice, I.C., Solomina, O., Stocker, T.F., Tarasov, P., Wagner, M., Widmann, M., 2008. Mid-to Late Holocene climate change: an overview. Quat. Sci. Rev. 27, 1791–1828.
Weber, W.A., 1976. Rocky Mountain Flora. Colorado Associated University Press, Boulder, CO.
Williams, A.P., Seager, R., Abatzoglou, J.T., Cook, B.I., Smerdon, J.E., Cook, E.R., 2015. Contribution of anthropogenic warming to California drought during 2012-2014. Geophys. Res. Lett. 42, 6819–6828.
Wise, E.K., 2012. Hydroclimatology of the US intermountain west. Prog. Phys. Geogr. 36 (4), 458–479.
Wolfe, A.P., Vinebrooke, R.D., Michelutti, N., Rivard, B., Das, B., 2006. Experimental calibration of lake-sediment spectral reflectance to chlorophyll *a* concentrations: Methodology and paleolimnological validation. J. Paleolimnol. 36 (1), 91–100.
Yackulic, E., 2017. Productivity and Temperature Variability over the Past 15000 Years at a Small Alpine Lake in the Southern San Juan Mountains, Colorado. MS Thesis. Northern Arizona University, Flagstaff.
Yuan, F., Koran, M.R., Valdez, A., 2013. Late glacial and Holocene record of climatic change in the southern Rocky Mountains from sediments in San Luis Lake, Colorado, USA. Palaeogeogr. Palaeoclimatol. Palaeoecol. 392, 146–160.